State of Health Estimation System for Lead-Acid Car Batteries

Through Cranking Voltage Monitoring

Ji Hoon Hyun

Thesis submitted to the faculty of the
Virginia Polytechnic Institute and State University
in partial fulfillment of the requirements for the degree of

Master of Science
In
Electrical Engineering

Dong S. Ha, Chair
Kwang-Jin Koh
Qiang Li

June 9, 2016
Blacksburg, Virginia

Keywords: Lead-Acid Battery, State of Health, State of Charge

State of Health Estimation System for Lead-Acid Car Batteries Through Cranking Voltage Monitoring

Ji Hoon Hyun

Abstract

The work in this thesis is focused on the development and validation of an automotive battery monitoring system that estimates the health of a lead-acid battery during engine cranking and provides a low state of health (SOH) warning of potential battery failure. A reliable SOH estimation should assist users in preventing a sudden battery failure and planning for battery replacement in a timely manner.

Most commercial battery health estimation systems use the impedance of a battery to estimate the SOH with battery voltage and current; however, using a current sensor increases the installation cost of a system due to parts and labor. The battery SOH estimation method with the battery terminal voltage during engine cranking was previously proposed. The proposed SOH estimation system intends to improve existing methods. The proposed method requires battery voltages and temperature for a reliable SOH estimation. Without the need for a costly current sensor, the proposed SOH monitoring system is cost-effective and useful for automotive applications.

Measurement results presented in this thesis show that the proposed SOH monitoring system is more effective in evaluating the health of a lead-acid battery than existing methods. A low power microcontroller equipped prototype implements the proposed SOH algorithm on a high performance ARM Cortex-M4F based MCU, TM4C123GH6PM. The power dissipation of the final prototype is approximately 144 mW during an active state and 36 mW during a sleep state.

With the reliability of the proposed method and low power dissipation of the prototype, the proposed system is suitable for an on-board battery monitoring as there is no on-board warning that estimates the health of a battery in modern cars.

Acknowledgements

I would like to express my inmost gratitude to my advisor, Dr. Dong S Ha, for giving me the opportunity to conduct this research. I am thankful to him for his endless support, insightful guidance, and motivation throughout the completion of this thesis.

I am also sincerely grateful to Dr. Kwang-Jin Koh and Dr. Qiang Li for their precious time and effort in reviewing my thesis and serving my thesis committee.

I would also like to express my thanks to Hyuk Jung, Cory Latham, Alex LePelch, and Daulet Talapkaliyev for their valuable assistance with the battery testing process and SOH algorithm implementation.

I appreciate Interstate Batteries in Salem, Virginia for providing me refurbished batteries used for battery aging and testing.

I am very grateful to my family and friends. Without their support, all of my academic accomplishments would not have been possible. Finally, I want to express my deepest love and thanks to my lovely wife, Julia, and my daughter, Ellie, for their unconditional love and constant encouragement during the entire process.

This work was supported in part by the Center for Integrated Smart Sensors funded by the Korea Ministry of Science, ICT & Future Planning as Global Frontier Project (CISS-2-3).

Table of Contents

List of Figures

List of Tables

1 Introduction

The lead-acid battery is still the most common rechargeable battery available on the automotive market due to its low cost with good performance, low maintenance requirements, low self-discharge rate with 2% to 3% loss per month, wide operating temperature range of -40 °C to 60 °C, and mature technology with more than 140 years of development [1, 2].

Lead-acid batteries have been widely used in automotive applications, and the gasoline-powered cars often use starting, lighting, and ignition (SLI) batteries to provide a large burst of current for a short period of time to start their engines [3]. This thesis explores several existing methods of state of health (SOH) estimation for lead-acid SLI batteries and presents a reliable method for the battery SOH estimation.

Electrical loads require more power from a battery in modern cars due to increased number of automotive electronics, such as in-car entertainment systems and on-board camera systems. Furthermore, many of modern cars automatically switch off their engines at stop-lights with the auto stop-start technology [4]. In other words, monitoring the health of a car battery becomes more important as cars become more advanced. While modern cars are equipped with various sensors for warning such as charging system warning and low tire pressure warning, currently there is no on-board warning that can prevent a sudden battery failure.

This thesis presents an on-board SOH monitoring system that estimates the health of a lead-acid battery during engine cranking and provides an advance warning several weeks prior to battery failure. It is advantageous that the proposed battery monitoring system is applicable to any type of a car equipped with a 12-volt lead-acid battery. Replacing an unhealthy battery with a low SOH

warning before the battery fails to start a car reduces unnecessary battery replacement and maintenance costs.

The organization of the thesis is as follows. Chapter 2 explores existing methods of automotive battery SOH estimation and their shortcomings. Chapter 3 describes the proposed automotive lead-acid battery SOH estimation method. Threshold development procedures for SOH estimation, battery SOC estimation, and experimental setup are also described briefly. Chapter 4 explains the implementation of the system with the proposed SOH monitoring algorithm embedded on a hardware prototype. Chapter 5 presents power dissipation of the system as well as battery test results with the proposed SOH monitoring system and ten lead-acid batteries. The battery test results are compared to other existing SOH estimation methods in this chapter. Chapter 6 draws a conclusion with future improvements.

2 Preliminaries

The battery SOH is a figure of merit implying the condition of a battery and related to its energy storing and current-delivering abilities, however there is no standardized metric [5]. For a vehicle with a lead-acid battery, it is important to estimate and monitor the SOH with a high reliability so one can estimate when to charge or replace the battery before battery failure. Replacing an unhealthy battery with a low SOH on time can avoid walk-home situations and eliminate unnecessary maintenance cost and efforts.

2.1 Impedance Based SOH Estimation Methods

In recent years, electrochemical impedance spectroscopy (EIS) has been used by battery manufacturers and automotive service centers to estimate the remaining life span of a lead-acid battery due to its reliability [6]. EIS is an effective technique for understanding the behavior of electrochemical power sources. For automotive applications, EIS measures the internal impedance of a battery in the frequency domain for the battery SOH estimation [7].

Grube investigated the characteristics of battery voltage and load current during engine cranking, and he confirmed that the relationship between voltage and current can be used to infer the condition of a lead-acid battery. Figure 1 (a) shows the relationship between battery voltage and load current of a healthy lead-acid battery during engine cranking. The battery voltage is linearly proportional to the current drawn to the load; however, this relationship tends to become non-linear as the battery becomes aged or unhealthy as shown in Figure 1 (b) [8].

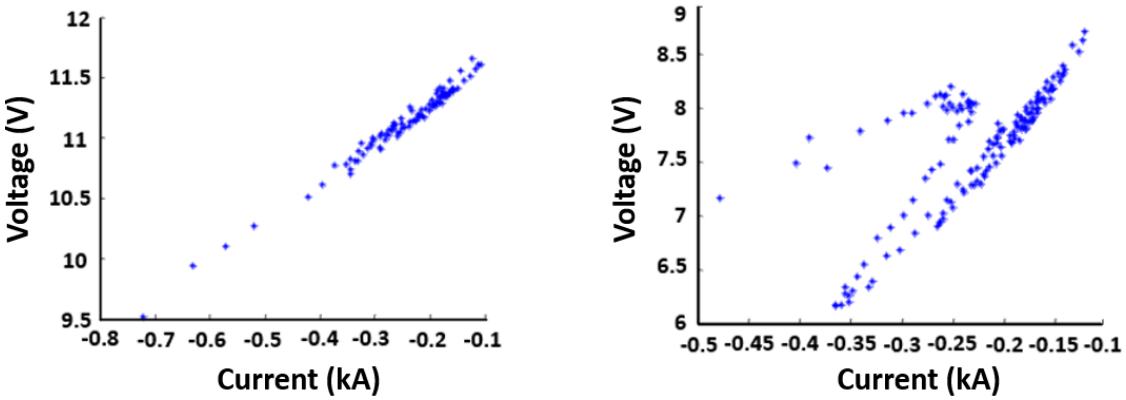

(a) Healthy battery *(b) Unhealthy battery*

Figure 1: Impedance characteristics of healthy (left) and unhealthy (right) batteries [8].

While the shape of the battery impedance has a strong correlation with the age of a lead-acid battery, the SOH estimation technique with EIS requires a costly current sensor with typically 10 mA current resolution over a wide range from 0.1 A to 1000 A, which increases installation cost and effort due to additional parts and labor [9]. Since the use of a current sensor makes the SOH estimation system costly, commercial SOH estimation products are often used by an automotive service professional or for research purposes [10].

2.2 Cranking Voltage Based SOH Estimation Methods

Grube observed that there is a relationship between battery cranking voltage characteristics and cranking power capability in lead-acid batteries [8]. Figure 2 (a) and (b) show typical voltage waveforms of healthy and unhealthy batteries.

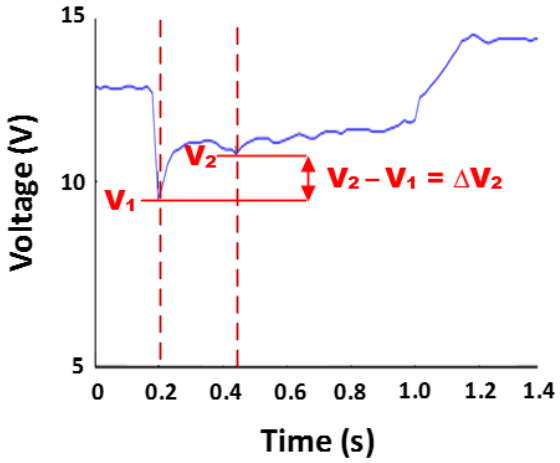

(a) Healthy battery

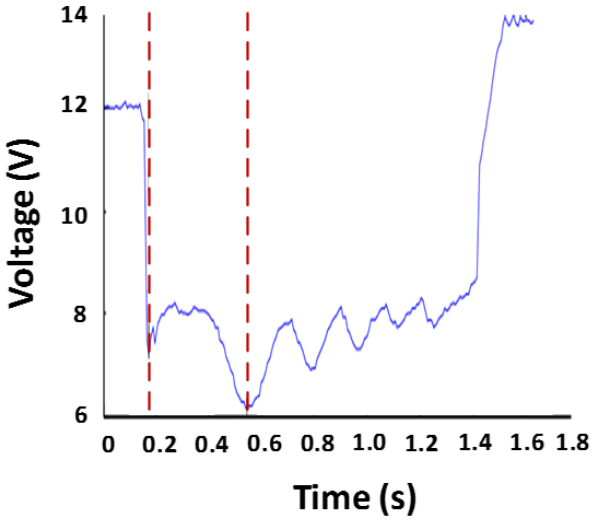

(b) Unhealthy battery

Figure 2: Voltage characteristics of healthy (top) and unhealthy (bottom) batteries [8].

It should be noted that the battery cranking voltage waveforms shown in Figure 2 (a) and Figure 2 (b) correspond to the voltage waveforms shown in Figure 1 (a) and Figure 1 (b) respectively. For an unhealthy battery as shown in Figure 2 (b), the second valley voltage, denoted as V_2 in Figure 2 (a), is smaller than the first valley voltage, denoted as V_1 in Figure 2 (a) due to the low cranking power capability of the battery.

In fact, Grube's cranking voltage based SOH estimation method exploits the difference between the first two valley voltages during engine cranking to estimate the SOH of a lead-acid battery. Grube's algorithm compares the difference between two valley voltages, denoted as ΔV_2 in Figure 2 (a), with a fixed threshold of 0.7 V for the SOH estimation. According to his algorithm, the battery is considered unhealthy if ΔV_2 is less than 0.7 V.

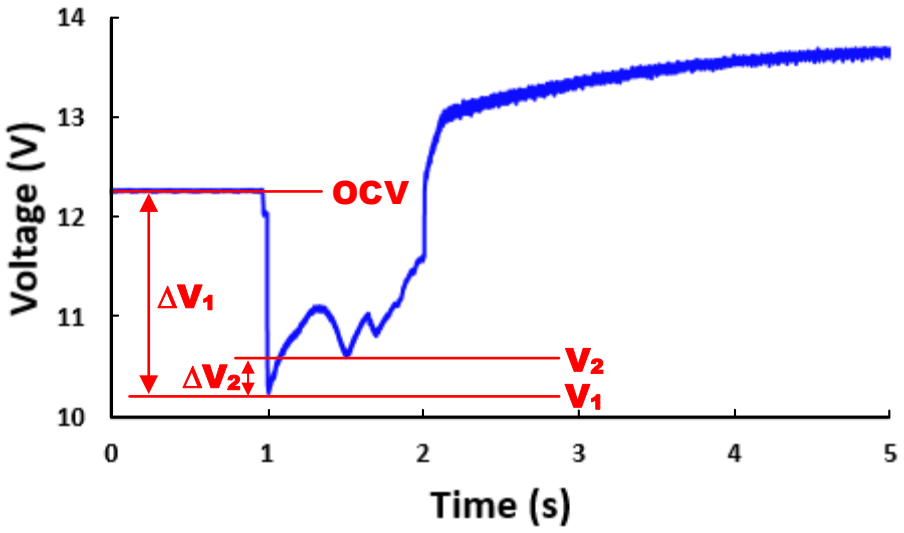

Figure 3: Typical cranking voltage waveform.

Although Grube's SOH algorithm provides an appropriate warning for an unhealthy battery without the need for a costly current sensor, his fixed threshold voltage does not account for the effect of an initial voltage drop (denoted as ΔV_1 in Figure 3) and battery temperature for the SOH estimation [8]. With a fixed threshold voltage, a battery estimated unhealthy could be estimated healthy on another day due to different internal or external battery conditions.

Kerley improved Grube's existing cranking voltage based SOH estimation method by incorporating the initial voltage drop and battery temperature in addition to the first two valley voltages. Kerley's algorithm determines two individual threshold voltages from lookup tables based on the two parameters, ΔV_1 and temperature. Once the two threshold voltages are

determined after a cranking event, the sum of the threshold voltages (V_{th}) is compared with a ΔV_2 for the SOH estimation. Based on his algorithm, a battery is considered unhealthy if ΔV_2 is less than the value of V_{th} [11, 12].

Kerley's measurement results show that his algorithm with the prototype works for the SOH estimation of lead-acid batteries, however his method does not take the state of charge (SOC) of a battery into consideration. It should be noted that the SOC is available battery capacity over nominal battery capacity, usually expressed as a percentage of nominal capacity [13]. Since the battery SOC is a critical parameter to consider as the performance of a battery with a low SOC is similar to the one of a falling battery, it is desired to consider the battery SOC for the battery SOH estimation. Moreover, both Grube's method and Kerley's method are based on a fully charged battery, and their methods become unreliable when the SOC of battery is low [11].

.

3 Proposed SOH Estimation Approach

This chapter presents the proposed SOH estimation method, battery SOC estimation, experimental setup including battery aging and testing, and the development of threshold voltages for the SOH estimation of lead-acid batteries.

3.1 Proposed Method

The proposed method addresses the shortcomings of the previous cranking voltage based SOH estimation methods by considering SOC, ΔV_1, ΔV_2, and battery temperature. The purpose of taking the battery SOC into account is to develop a more reliable SOH estimation method. By considering the SOC of a battery, the SOH estimation should distinguish a battery with a low SOC from an unhealthy battery so one can simply charge the battery and avoid unnecessary battery replacement. The proposed algorithm uses three individual threshold voltages from ΔV_1, SOC, and temperature for the SOH estimation. With the proposed SOH estimation method, a battery is considered healthy if ΔV_2 is greater than the sum of the three threshold voltages, V_{th}.

3.2 Battery SOC Estimation

The SOC of a battery is a function of a specific gravity as shown in Figure 4, and the specific gravity is a function of battery open-circuit voltage and battery temperature [2, 14]. In other words, the battery SOC can be determined from two parameters, battery open-circuit voltage (OCV) and temperature. The OCV is a battery terminal voltage after the battery voltage is settled, and the battery terminal voltage is considered settled when the difference between the maximum battery voltage and minimum battery voltage in 60 minutes is less than 0.1 V for this work. For lead-acid

batteries, the specific gravity is defined as the concentration of sulfuric acid electrolyte relative to the concentration of water at a given temperature, and it is highest in a fully charged battery [15].

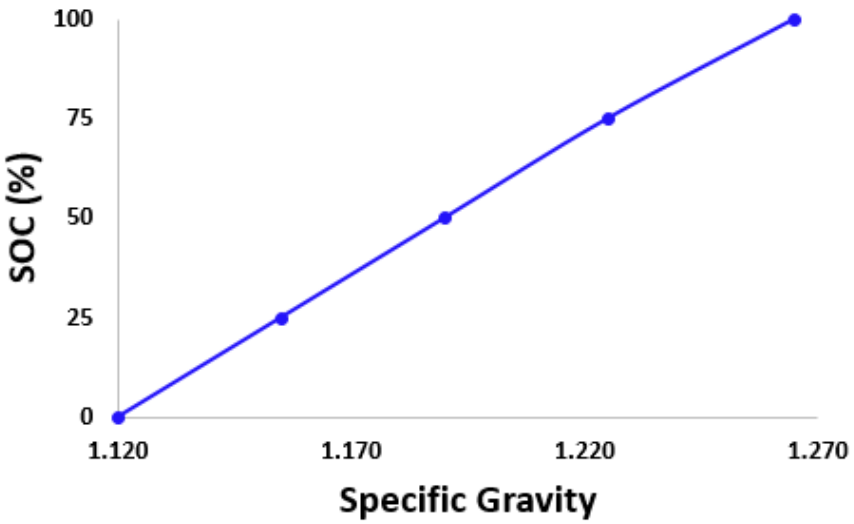

Figure 4: Battery SOC as a function of specific gravity [2].

Figure 5 shows a relationship between the cell voltage and the specific gravity of a lead-acid battery at 25 °C [14]. Since a lead-acid battery has six cells connected in series inside the battery container, a true OCV is six times the battery cell voltage. Therefore, a specific gravity of a lead-acid battery can be estimated with a measured OCV assuming the OCV is measured at 25 °C.

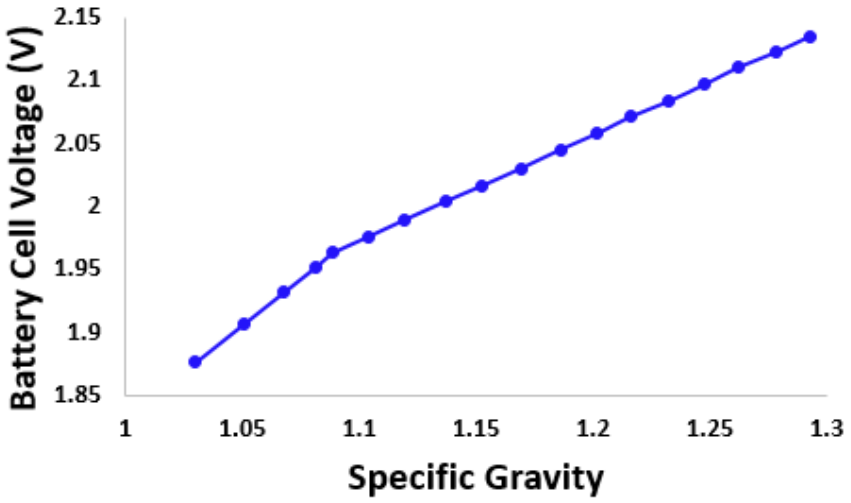

Figure 5: Battery cell voltage as a function of specific gravity at 25 °C [14].

Since the specific gravity is a function of OCV and battery temperature, it is necessary to consider the temperature of a battery ($T_{battery}$) for the SOC estimation. Once the specific gravity of a battery is determined from the measured OCV, the temperature coefficient (TC) of the measured OCV can be estimated from Figure 6.

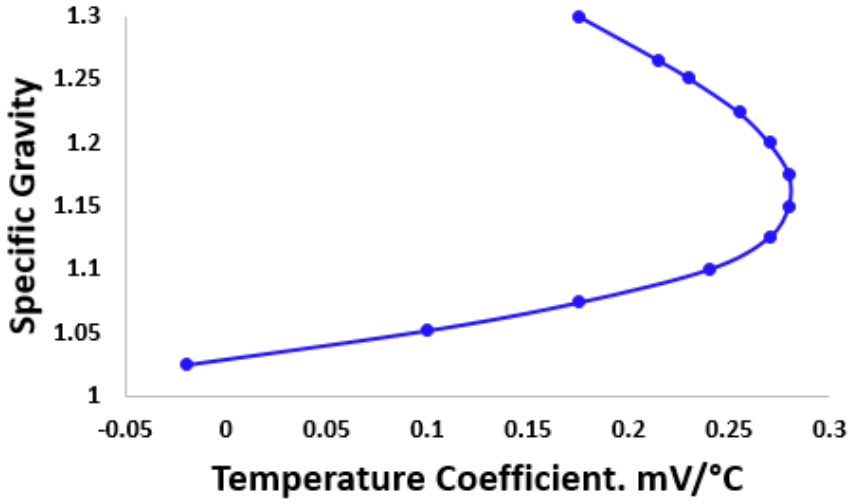

Figure 6: Temperature coefficient of OCV as a function of specific gravity at 25 °C [2].

It is important to note that both Figure 5 and Figure 6 assume that the battery OCV is measured at 25 °C, which makes the following equation legitimate [2, 14, 16].

$$OCV_{25\,℃} = OCV_{measured} + 6 \cdot [(T_{battery} - 25\,℃) \cdot (1000 \cdot TC)] \quad (1)$$

With the equation shown above, the OCV at the temperature of 25 °C can be estimated with a measured OCV at any given battery temperature; for example, if a measured OCV is 12.6 V at 20 °C, the estimated value of $OCV_{25\,℃}$ will be 12.5 V according to the equation, Figure 5, and Figure 6. When the OCV at 25 °C is determined, a battery SOC can be estimated based on Figure 4 and Figure 5. For the example given above, the battery SOC is 90%. The values from Figure 4 to Figure 6 are extracted and used in the algorithm developed in the Energia environment with a TI EK-TM4C123GXL evaluation board to estimate the SOC of a lead-acid battery [17].

3.3 Experimental Setup

Since typical lead-acid batteries for vehicles last four to five years before requiring replacement, an accelerated aging process is desired to observe and analyze the battery characteristics in a short period of time until the battery is no longer able to start a car [18]. In order to develop the three threshold voltages, it is necessary to obtain cranking waveforms and temperature data of each battery after aging and testing. For the experiment, three new batteries and seven refurbished batteries are aged with repeated charging and discharging and tested on a car to obtain cranking voltages and temperature data.

3.3.1 Battery Aging and Testing Procedures

The SAE J240 life test for automotive storage batteries published by the Society of Automotive Engineers has become a widely used and trusted life test for battery aging. Even though the recommended test temperature is 40 °C in the original test procedure, a higher test temperature at 75 °C is also acceptable and can accelerate the battery aging to further decrease the lifetime of the battery [19]. For this research work, the following battery aging and testing procedures for ten lead-acid batteries are derived from the SAE J240:

1. During the battery aging process, each battery is submerged in a water bath maintained at 75 °C for faster chemical reactions.
2. Each battery is charged at 14.8 V for 10 minutes and discharged at 8 V for 5 minutes with a maximum current of 25 A, and this charging and discharging process is continuously cycled for 100 hours.

3. After 100 hours of battery aging with charging and discharging, each battery is charged for 10 to 12 hours followed by an open-circuit relaxation for up to 24 hours to allow the battery terminal voltage to settle.
4. Once the aging and charging process is complete, each battery is tested on a car with engine cranking. The voltage and temperature data of each cranking event are collected for the development of the threshold voltages.
5. Procedures from 1 to 4 are repeated until each battery fails to start a car.

3.3.2 Battery Aging Test Bench

The battery aging test bench used for charging and discharging ten lead-acid batteries is shown in Figure 7. Ten batteries are submerged in a 110-gallon water bath. The water level of the bath is maintained at approximately 75% of the battery container height. A 1.5 kW immersion heater [20], as shown on the bottom left corner in the figure, is used with commercial temperature controller and thermocouple to maintain the water temperature at 75 °C. Three submersible water pumps are also used to circulate the heated water evenly in the bath.

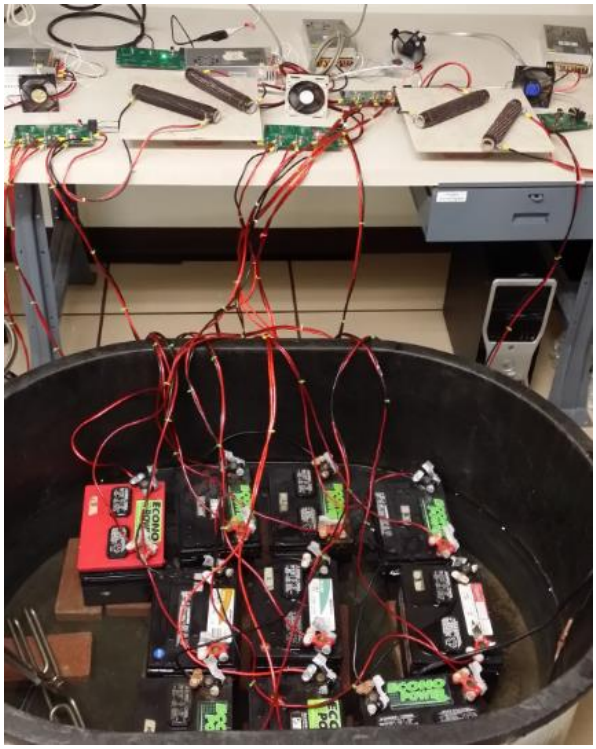

Figure 7: Battery aging test bench.

Whenever battery aging takes place, the water bath is covered with a polystyrene foam board on the top and foam insulation sheets on the side as shown in Figure 8 in order to minimize heat loss and water evaporation.

Figure 8: Insulated battery water bath.

A custom PCB with a TI MSP430G2553 microcontroller serves as an automated battery cycler [21], as shown in Figure 9, to age up to three batteries with a DC power supply unit (PSU) and 0.5 Ω 300 W wire-wound resistor. As ten lead-acid batteries were used for this research work, four battery cyclers have been used. A simplified diagram of the battery cycler is depicted in Figure 10.

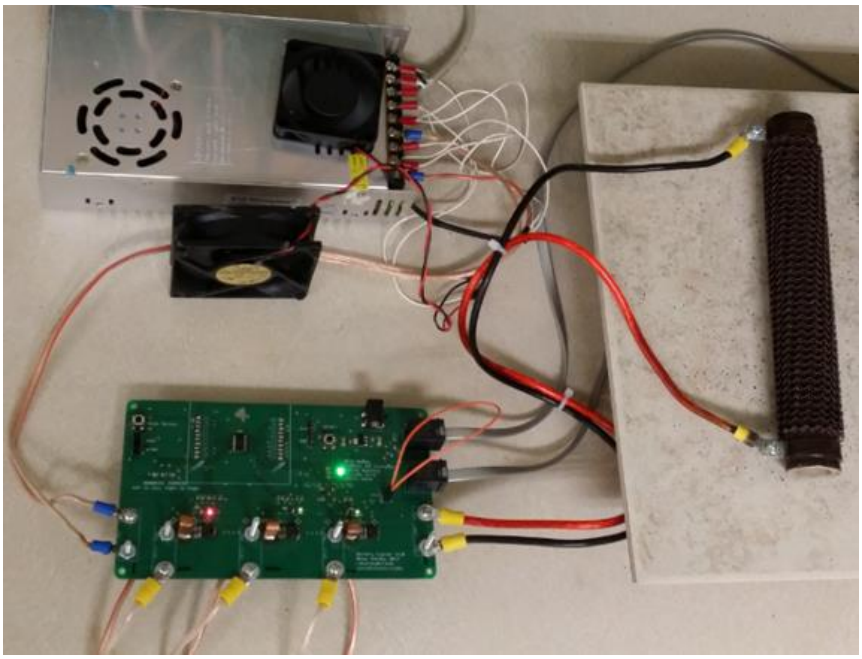

Figure 9: Automated battery cycler.

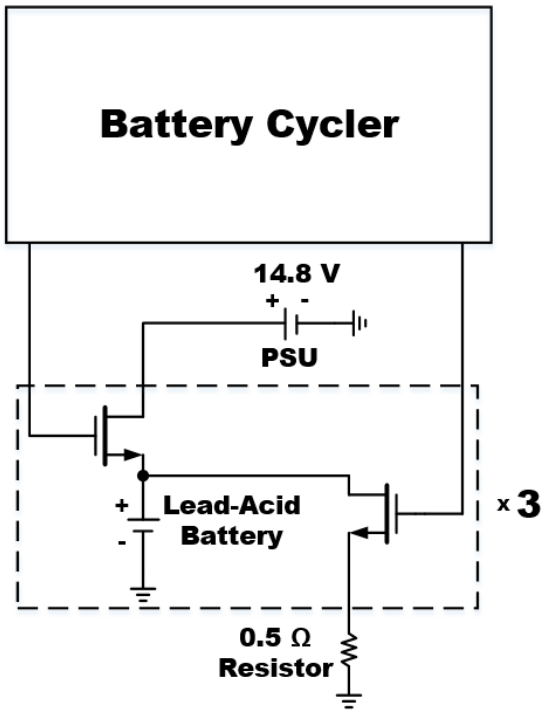

Figure 10: Simplified diagram of a battery cycler.

It should be noted that the battery cycler has six load switches (VN5E010MH-E) surface mounted on the board [22]. Due to the heat dissipation of the load switches on the battery cyclers, copper heat sinks as well as a fan for each battery cycler are used to avoid any excessive heat. An analog current pin of the load switch is capable of sensing charging and discharging current of a battery. Each battery cycler charges two batteries and discharges one battery at the same time during battery aging, and voltage and current measurements of each battery are sent over to the host PC through I^2C with a master board including a TI MSP430G2553 microcontroller to make sure that each battery is aged appropriately [21]. Figure 11 illustrates the block diagram of the battery aging test bench that ages ten lead-acid batteries. Since ten batteries were used and each battery cycler can handle up to three batteries at a time, one of the battery cyclers was used to age only one battery.

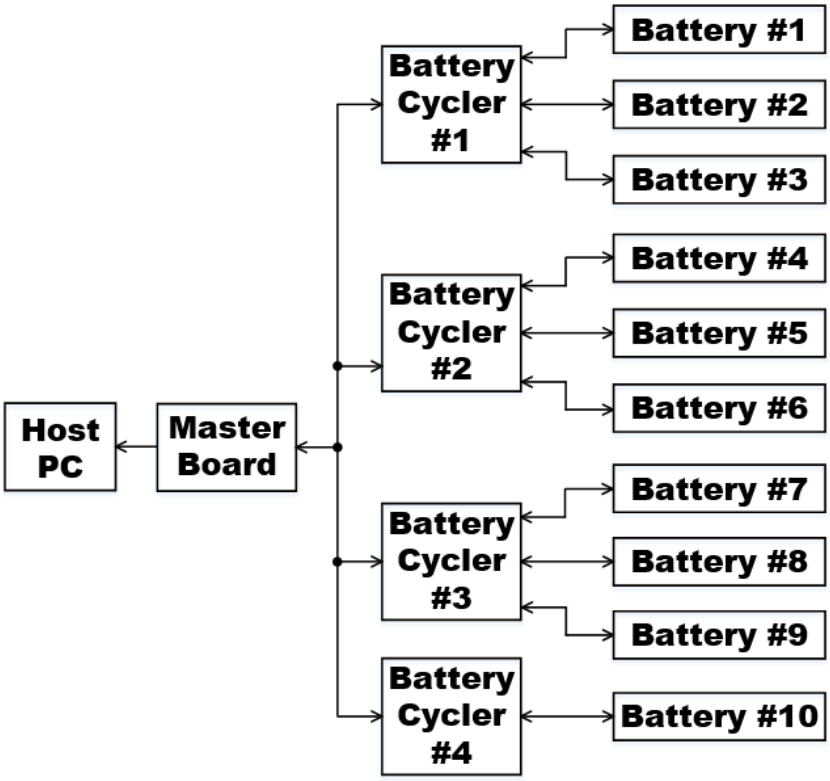

Figure 11: Block diagram of battery aging test bench.

Figure 12 shows voltage and current data during battery aging. Each lead-acid battery is charged at above 14 V for 10 minutes with the power supply and discharged approximately at 8 V for 5 minutes with the resistor.

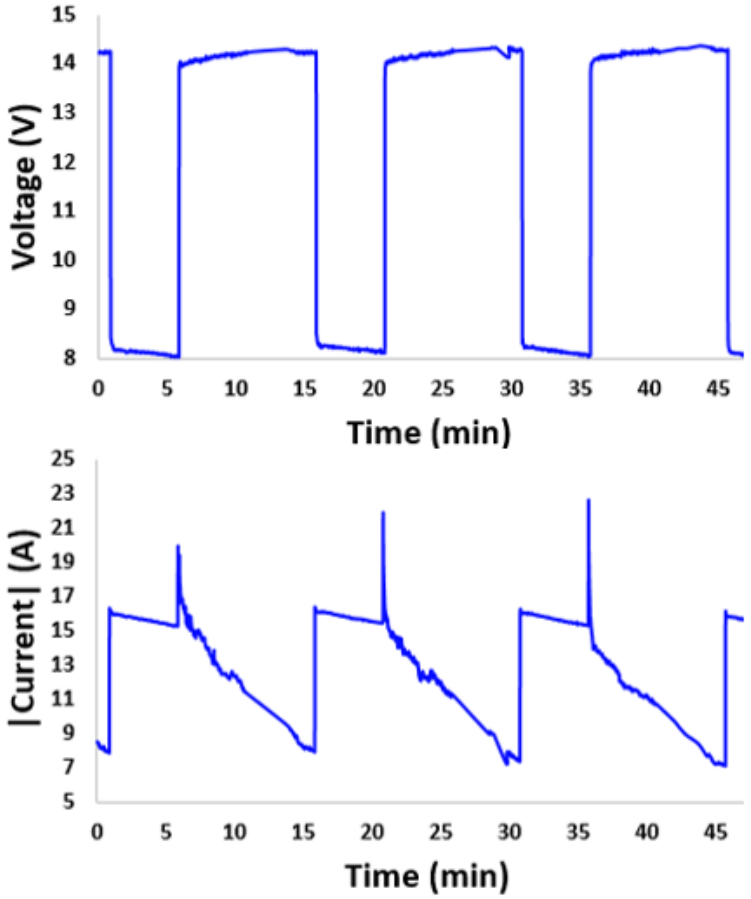

Figure 12: Voltage and current measurements during battery aging.

The discharging current flowing from the battery to the resistor is approximately 16 A while the charging current flowing into the battery from the power supply begins with up to 23 A and gradually decreases to 7 A as the battery becomes more charged as shown in the figure above. Thus, both charging and discharging currents do not exceed 25 A.

3.3.3 Battery Test and Data Collection

After the battery aging process is complete for each battery, the battery is installed on a car for testing. During engine cranking with the aged battery, battery voltage and battery temperature were collected with a USB oscilloscope (Analog Discovery by Digilent [23]) and digital thermometer (TMD-56 by Amprobe [24]) for data logging. The sampling rate for battery voltage sensing with

the oscilloscope is configured at 10 kHz, and this sampling rate is more than sufficient for data analysis.

Before engine cranking is performed, a commercial battery tester (PBT-300 by Midtronics) is also used to test each battery. The PBT-300 can estimate the health of a lead-acid battery based on the conductance of the battery and provide warnings if the battery is healthy, low in charge, or unhealthy [25]. Once the aging process and battery charging is complete, each battery is tested on a car with engine cranking as shown in Figure 13. The voltage and temperature measurements of each cranking event are recorded for the development of the threshold voltages.

Figure 13: Battery testing on a car and data collection.

Battery cranking waveforms of battery #10 is shown in Figure 14; it is important to note that there is approximately a week of battery aging between two consecutive battery tests, and the batteries are tested at the end of each battery aging and charging. The OCV of each battery test varies depending on how long the battery is charged before the test, and different OCV of a battery at a

given temperature causes the battery to have a different SOC at the time of a battery test. It is indeed important to test a battery with a different SOC to investigate the effect of the battery SOC on the SOH estimation.

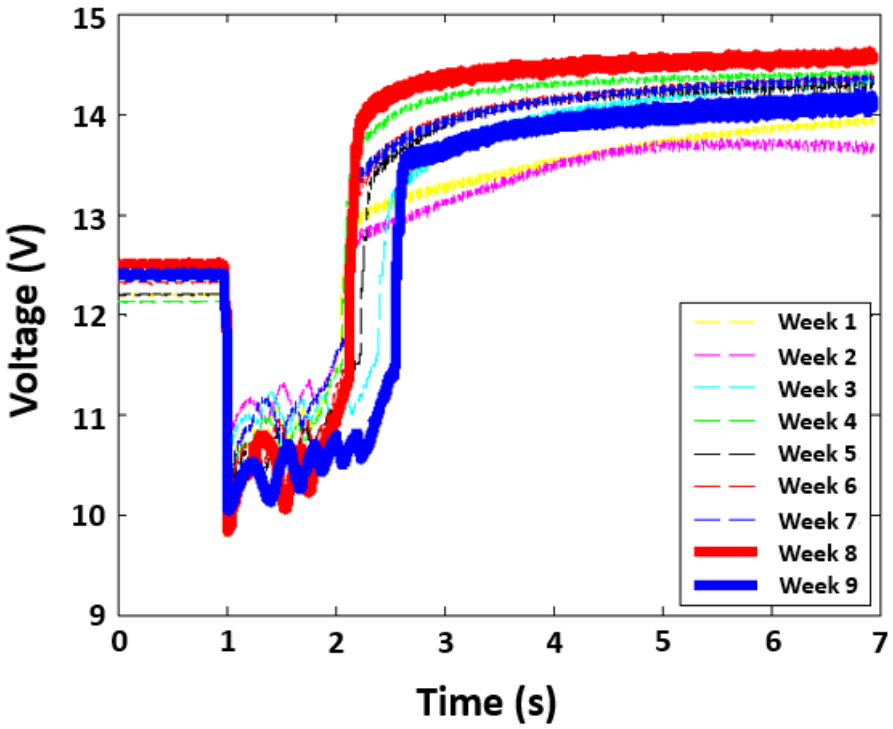

Figure 14: Battery cranking voltage waveforms of battery #10.

Table 1 summarizes the data associated with each engine cranking of battery #10. Based on the table shown below, it can be observed that the initial voltage drop (ΔV_1) tends to increase and the first two valley voltages tend to decrease as the number of aging periods increases. The objective of the proposed SOH estimation is to provide a low SOH warning near the end of battery life. In such a way, the battery is still able to start a car, but the battery is estimated to be unhealthy so the user can have the battery checked by an automotive service professional or replace the battery in advance before battery failure. The measured data and test results are available in Appendix A: Battery Measurements and Test Results.

Table 1: Measured data from battery #10.

Period	°C	OCV (V)	SOC (%)	V_1 (V)	V_2 (V)	ΔV_1 (V)	ΔV_2 (V)	Pass/Fail
Week 1	27.1	12.20	37	10.46	10.70	1.74	0.24	Passed
Week 2	12.4	12.39	65	10.85	10.94	1.54	0.09	Passed
Week 3	8.0	12.37	63	10.72	10.93	1.65	0.21	Passed
Week 4	6.3	12.14	31	10.42	10.63	1.72	0.21	Passed
Week 5	7.6	12.20	39	10.34	10.46	1.86	0.12	Passed
Week 6	9.1	12.32	56	10.33	10.55	1.99	0.22	Passed
Week 7	5.3	12.52	83	10.39	10.76	2.13	0.37	Passed
Week 8	7.9	12.51	82	9.96	10.11	2.55	0.15	Passed
Week 9	20.8	12.39	63	10.13	10.17	2.26	0.04	Passed
Week 10	21.4	10.39	0	N/A	N/A	N/A	N/A	Failed

3.4 Threshold Development

For this research work, the following procedures are adopted for the development of the three threshold voltages (V_{th1}, V_{th2}, and V_{th3}):

1. Develop threshold slopes based on the aging data of the three new batteries.
2. Fine tune the threshold values using the data from ten batteries.

3.4.1 ΔV_1-dependent Threshold (V_{th1})

The effect of battery aging is considered for the threshold development initially because the trend of the ΔV_1 values with battery aging can be identified conveniently. Individual ΔV_1 values of the three new batteries as a function of battery aging from week 1 to week 10 are shown in Figure 15. Based on the collected data as shown in the figure below, the initial voltage drop generally increases as the battery becomes more aged.

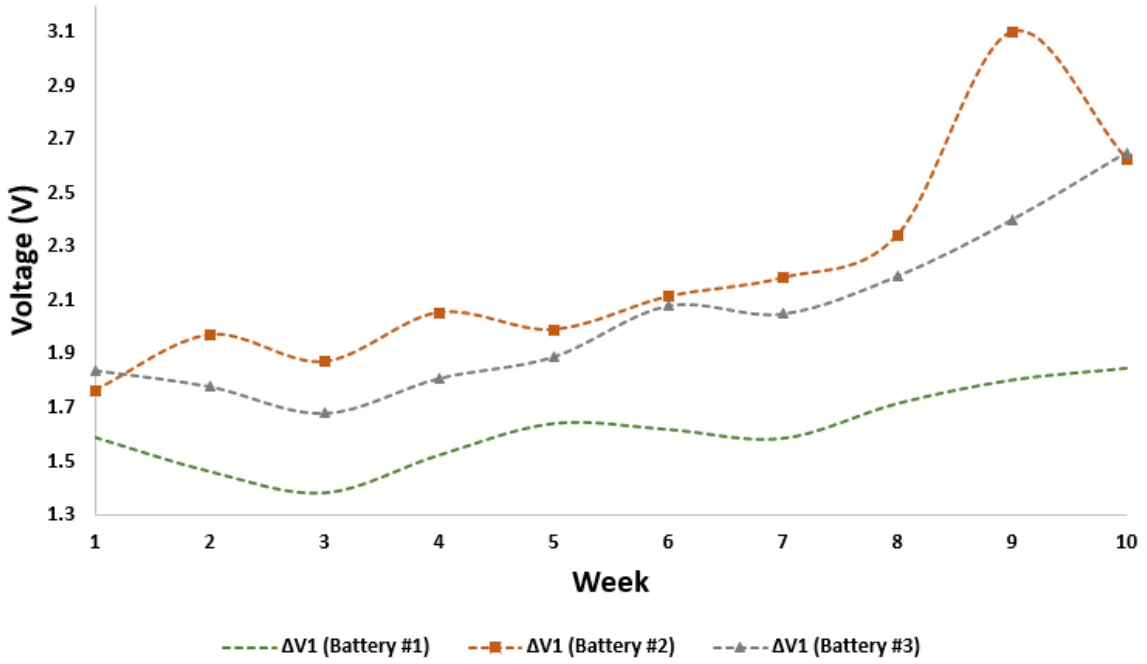

Figure 15: Individual ΔV_1 of three new batteries as a function of battery aging.

Since the typical initial voltage drop of a nearly new battery is 1.6 V based on the collected data, a threshold slope is developed as shown in Figure 16. When the threshold is set higher for a larger ΔV_1, it can prevent the case where a battery is incorrectly estimated to be healthy with a large initial voltage drop since a large V_{th1} implies that a battery is more aged. Positive threshold voltages are assigned to the initial voltage drops greater than 1.6 V so smaller SOH values can be assigned to more aged batteries. V_{th1} is set to linear to ΔV_1, and it is developed by examining data from battery tests. The scale of the threshold values is based on the scale of ΔV_1 values after comparing the collected data from ten lead-acid batteries. The threshold voltages used in the figure below are the final values used to satisfy the measurement data collected from all the batteries.

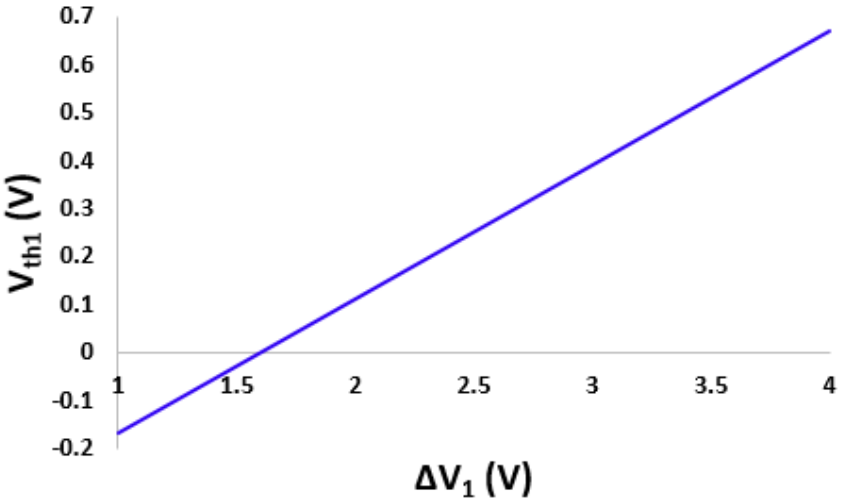

Figure 16: V_{th1} as a function of ΔV_1.

Figure 17 shows the original ΔV_2 values as well as SOH values with only the ΔV_1-dependent thresholds considered for the SOH estimation of battery #3. Based on the figure, the battery is healthy all the time if the ΔV_1-dependent thresholds are not considered. In the figure, a battery is considered unhealthy if an SOH value ($\Delta V_2 - V_{th1}$) is negative. By taking the ΔV_1-dependent thresholds into account, the battery can be estimated as unhealthy at week 2, 5, 9, and 10. It is worth mentioning that the SOH values are negative at week 2 and 5 due to a low battery SOC, and it can be confirmed in Appendix A.

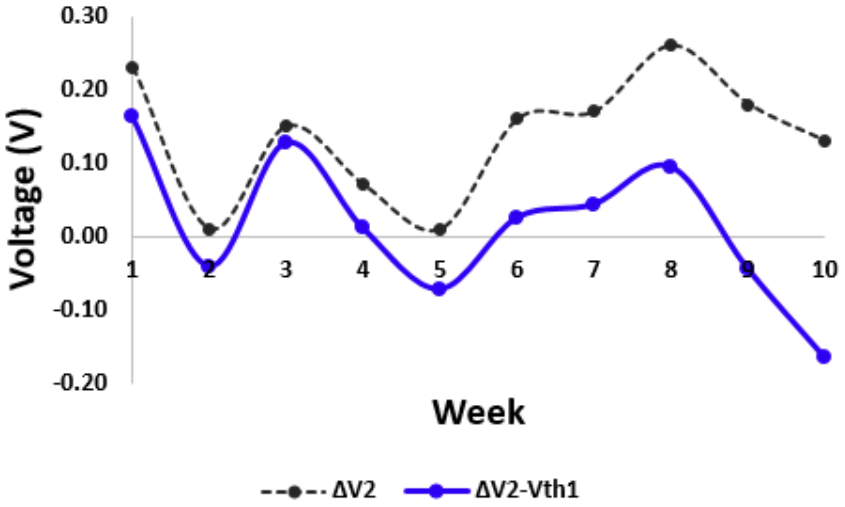

Figure 17: ΔV_2 and ΔV_2-V_{th1} as a function of battery aging for battery #3.

3.4.2 SOC-dependent Threshold (V_{th2})

As shown in Figure 17, it is possible that the battery can be incorrectly estimated unhealthy due to a low battery SOC. To prevent such cases, the SOC of the battery should be considered for the SOH estimation in addition to battery aging. Figure 18 shows SOC-dependent thresholds, V_{th2}. Since a fully charged battery should not be affected by V_{th2}, V_{th2} is set to zero for a fully charged battery. Negative threshold voltages are assigned to the SOC less than 100% because a battery with a low SOC should not fail if the battery is actually healthy. It is important to note that the performance of a healthy battery with a low SOC is similar to the one of an unhealthy battery. When the threshold is set lower for a lower SOC value, it can prevent the case where a battery is estimated to be healthy at high SOC but unhealthy at low SOC. The threshold voltages used in the figure below are the final values used for the battery SOH estimation after calibration.

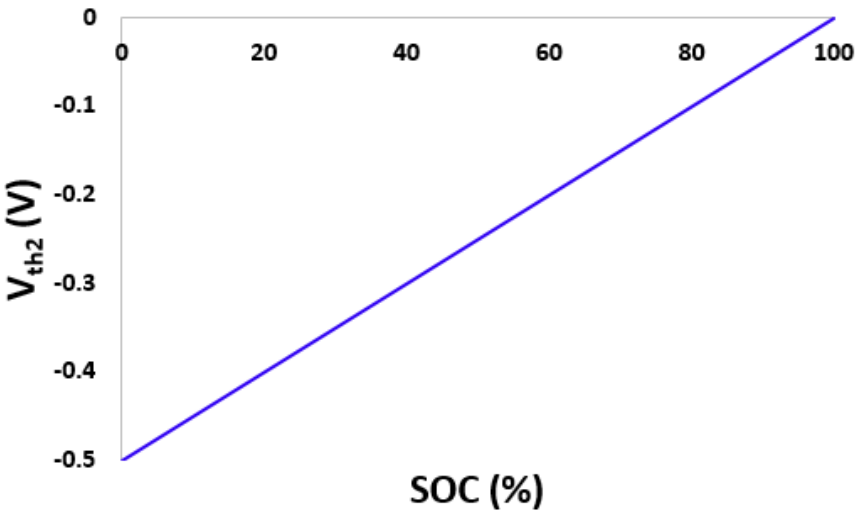

Figure 18: V_{th2} as a function of battery SOC.

Figure 19 shows SOH values considering only ΔV_1-dependent thresholds as well as SOH values considering both ΔV_1-dependent thresholds and SOC-dependent thresholds for the SOH estimation of battery #3. By considering SOC-dependent thresholds in addition to ΔV_1-dependent thresholds, the battery is healthy throughout the entire battery aging periods except the last week.

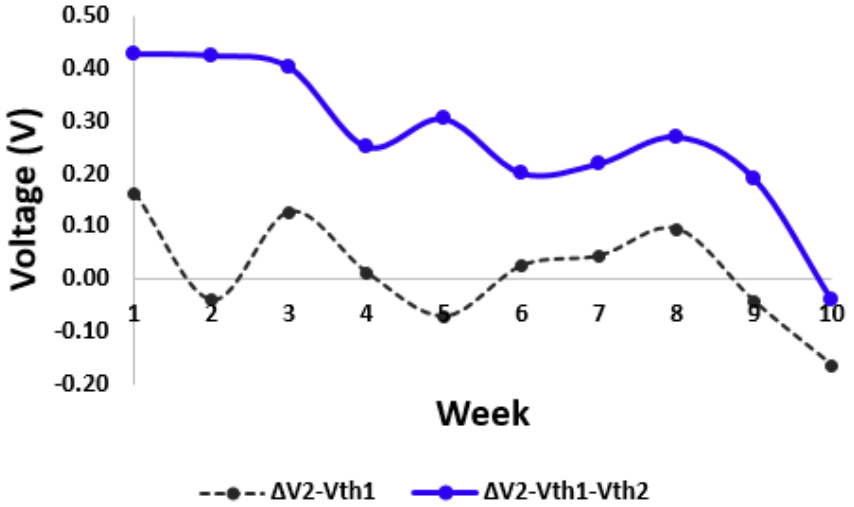

Figure 19: ΔV_2-V_{th1} and ΔV_2-V_{th1}-V_{th2} as a function of battery aging for battery #3.

3.4.3 Temperature-dependent Threshold (V_{th3})

Although the SOC of a battery takes temperature into consideration, a variation in the battery SOC due to temperature differences is insufficient to consider the effect of temperature on the SOH estimation. For example, with the measured battery voltage of 12.6 V, the SOC of the battery is 93% at 50 °C, while the SOC of the battery is 91% at 30 °C. To better match the measurement results, it is necessary to use an additional temperature compensation with temperature-dependent thresholds in addition to battery aging and battery SOC. Figure 20 shows temperature-dependent thresholds, V_{th3}. A battery tends to supply current better with low resistance due to fast chemical reactions at a higher temperature. When a threshold is set larger at a higher temperature, it can prevent the case where a battery is estimated to be healthy at a high temperature but unhealthy at a low temperature [14]. Positive thresholds are assigned to temperature above 0 °C, and the threshold values are developed by comparing the performance of the batteries tested. Threshold values below 0 °C are extrapolated. It should be noted that the threshold slope is set to decrease with the temperature increase to match the battery test results collected from the ten batteries.

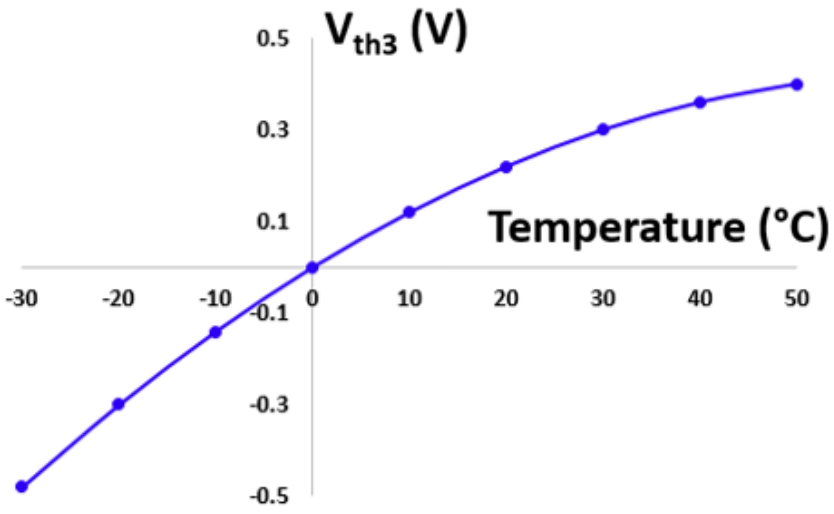

Figure 20: V_{th3} as a function of battery temperature.

After considering all three thresholds for the SOH estimation, the blue plot shown in Figure 21 can be obtained. Figure 21 shows SOH values considering both ΔV_1-dependent thresholds and SOC-dependent thresholds as well as SOH values considering all three thresholds for the SOH estimation of battery #3. It can be observed that the SOH values of the battery considering all three thresholds are relatively consistent until the fifth week, and the SOH values decreases afterwards. For week 10, the SOH value is negative. Therefore, a low SOH warning can be given during this period since the battery failed to start a car at week 11.

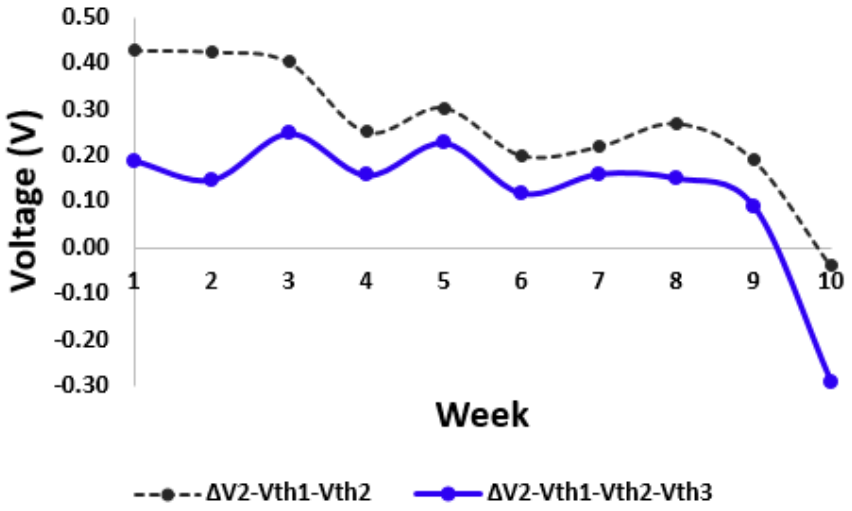

Figure 21: ΔV_2-V_{th1}-V_{th2} and ΔV_2-V_{th1}-V_{th2}-V_{th3} as a function of battery aging for battery #3.

With the threshold values developed for the SOH estimation, the health of ten lead-acid batteries could be accurately estimated as shown in Appendix A.

4 System Implementation

This chapter describes the system implementation of the SOH estimation method. A stand-alone battery SOH estimation system, SOH estimator, is developed with the proposed algorithm to provide a low SOH warning for an unhealthy battery and prevent a sudden battery failure.

4.1 System Block Diagram

Figure 22 depicts a proposed block diagram of the SOH estimator. Two analog-to-digital converters (ADCs) are to sense battery voltage and temperature, and the use of a dependable temperature sensor is essential for the battery SOC estimation. Since the active operation of the SOH estimation system is only necessary during engine cranking, the power dissipation of a microcontroller unit (MCU) can be optimized by making the MCU sleep when not required. The purpose of using an accelerometer is to wake up the MCU with a door activity, such as a door opening or closing. A step-down converter, buck converter, is to supply a required voltage for system blocks from a battery. Indicator LEDs are to indicate the condition of a battery and status of the prototype.

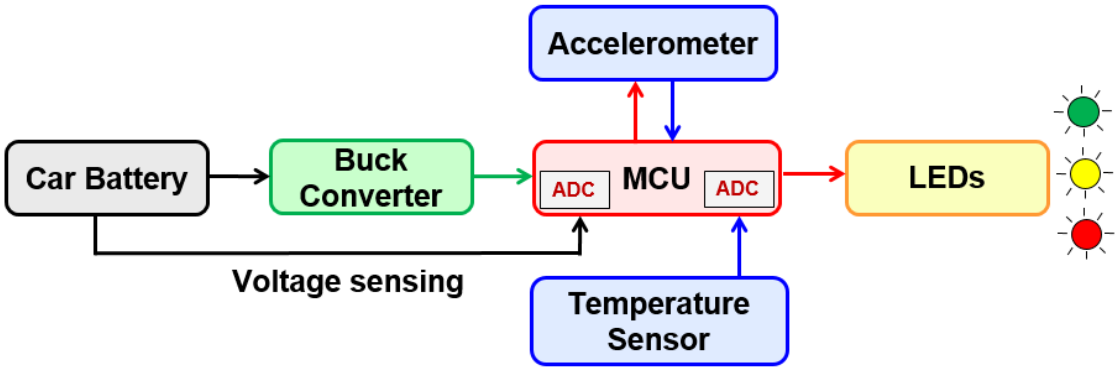

Figure 22: Block diagram of SOH estimator.

4.2 Hardware Prototypes

Two PCB prototypes are populated to validate and test the SOH algorithm. Figure 23 (a) shows a prototype that includes an SD card slot for data logging of battery tests with a TI EK-TM4C123GXL evaluation board equipped with two MCUs [17]. The evaluation board attached to the PCB board has an integrated in-circuit debug interface which allows programming and debugging of the prototype; however, this increases the power dissipation of the system as the two MCUs on the evaluation board operate at the same time during an active operation. The stand-alone prototype, SOH estimator, as shown in Figure 23 (b) has only one MCU to minimize the power dissipation of the system. For the stand-alone prototype, JTAG connectors are for programming and debugging the MCU, and UART connectors are for serial monitoring.

Both prototypes use the same type of MCU, temperature sensor, accelerometer, and buck converter. A high efficiency synchronous step-down converter, LTC3631 [26], converts the battery voltage to supply a 3.3 V for the MCU (TM4C123GH6PM [27]) and accelerometer (ADXL345 [28]). The TM4C123GH6PM used for the prototypes is an ARM Cortex M4F based MCU operating at a clock speed of 80 MHz with 256 KB of RAM, and the ADXL345 is a low power 3-axis accelerometer that supports an I^2C interface. An analog output temperature sensor, LM34, is powered by a car battery, and it provides typical accuracies of ±0.5 °F for the temperature range of -50 °F to 300 °F [29].

For the DC inputs of the prototypes, voltage divider and first-order RC low pass filter are included to sense battery voltages and reduce false valley detection due to noise. The ratio of the voltage divider is set to approximately 1/5 with the use of 10 KΩ and 39 KΩ resistors for battery voltage sensing since the maximum analog input voltage limit of the MCU's ADC is 3.3 V. For the low

pass filter, a 0.47 µF capacitor is placed in parallel to the 10 KΩ resistor to help noise reduction of the battery voltage. Three indicator LEDs (green, yellow, and red) are used to indicate if the MCU is awake and ready for engine cranking, a battery needs charging, or a battery is unhealthy.

The hibernation module embedded in the MCU allows the battery-backed memory to maintain up to sixteen 32-bit words during the sleep state so relevant parameters, such as recent OCV value and previous SOH values, can be retrieved upon wake-up for SOC and SOH estimation.

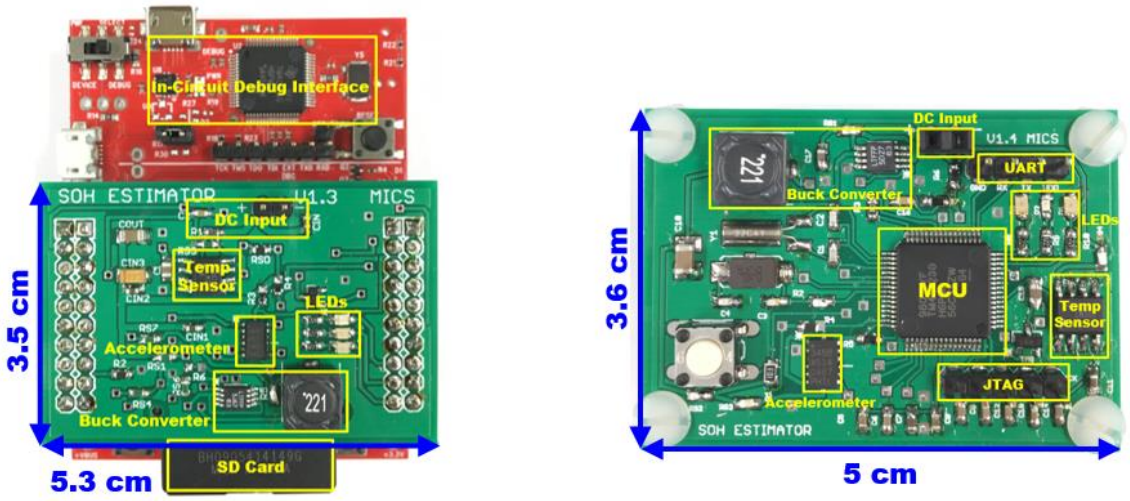

(a) Data logger prototype *(b) Stand-alone prototype*

Figure 23: Hardware Prototypes.

4.3 Proposed SOH Algorithm

For the stand-alone battery SOH estimation system that can repeatedly monitor the battery condition, the development of a robust battery SOH estimation algorithm is necessary to correctly estimate the health of a battery. The algorithm is developed in the Energia environment, and the total RAM usage of the proposed SOH estimation algorithm by voltage samples is approximately 12 KB.

4.3.1 Algorithm Overview

A decision path for the SOH estimation algorithm is shown in Figure 24. Once the prototype is connected to the battery terminals or constant 12-volt wires, such as alarm system or remote starter, with a frame ground on a car, the MCU waits until the battery voltage is settled to measure and store the OCV of a battery. For the battery SOC estimation, the MCU wakes up every 30 minutes to measure battery voltages, and the battery temperature is measured after a door activity is detected with the accelerometer. For the proposed algorithm, the battery voltage is considered settled when the difference between the maximum battery voltage and minimum battery voltage in 60 minutes is less than 0.1 V with the voltage range between 11 V and 13 V.

Once the OCV is settled and stored in a register in the MCU, the MCU enters its sleep state and waits for a user to open or close the car door since the accelerations due to a door activity can be detected by the accelerometer. Once the MCU is awake due to a door activity and battery voltage is settled, the green LED is turned on to notify the user to start a car for the SOH estimation. At the same time, the battery SOC is estimated with the battery temperature. The yellow LED will be turned on if the battery SOC is less than 40% so the user can charge the battery. The ADC of the MCU samples car battery voltages continuously and waits for a cranking event. To prevent a case where the user opens or closes the car door but does not start the car, the MCU is configured to detect a cranking event for 3 minutes before returning to the sleep state again. When a cranking event is detected while the MCU is awake, the MCU carries out the battery SOH estimation and gives a low SOH warning by turning on the red LED if four consecutive SOH values are negative.

After detecting a cranking event and estimating the SOH of a battery, the MCU is in the sleep state continuously unless the car is off. While the MCU is in the sleep state, the MCU wakes up every

10 minutes to sample the battery voltage to see if the voltage is below 13 V which will only be true when the user has turned off the car and the alternator is not charging the battery. When the battery voltage is sampled at below 13 V, the SOH algorithm cycle can be repeated once again and the MCU checks whether the battery OCV is settled or not.

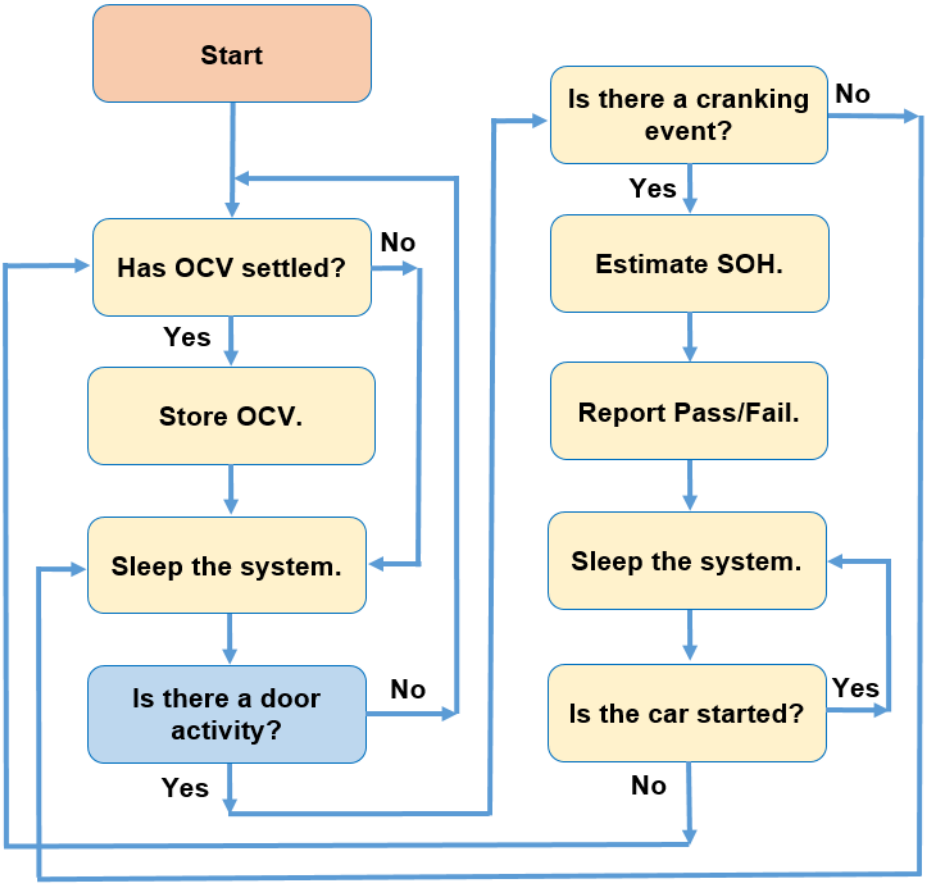

Figure 24: Decision path for proposed algorithm.

4.3.2 Voltage Sampling

The sampling rate is set to 200 Hz with 16-bit per sample for the prototypes, and this sampling rate is sufficient to correctly identify the first two valley voltages during engine cranking. Every five seconds, the MCU checks to see if there is a cranking event. When the cranking event is detected, the MCU processes the previous ten seconds of data for the SOH estimation. Ten seconds

of voltage samples is copied to a buffer array to allow the ADC to keep sampling without any interrupt. In addition to the low pass filter used for the prototypes to attenuate the high frequency noise of the battery voltage, a running average of four voltage samples from the copied array further reduces the possibility of false valley detection.

4.3.3 Cranking and Valley Detection

For robust SOH estimation, it is crucial to accurately detect a cranking event and as well as the first two valley voltages. Figure 25 illustrates a typical cranking voltage waveform of a lead-acid battery collected with the prototype for data logging.

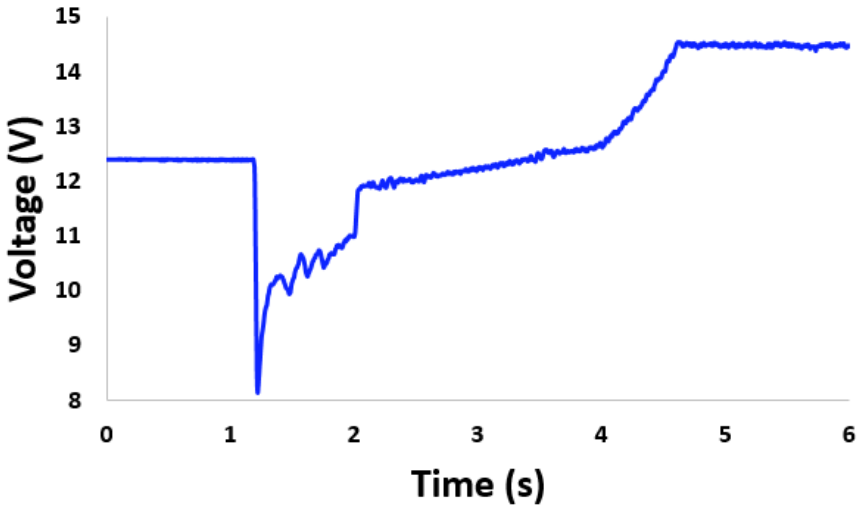

Figure 25: Typical cranking voltage waveform collected with data logger prototype.

The proposed algorithm detects a cranking event if the difference between two consecutive battery voltages is greater than 0.25 V as shown from the circled region of Figure 26. This cranking detection method is confirmed to detect engine cranking for all batteries tested with the prototypes.

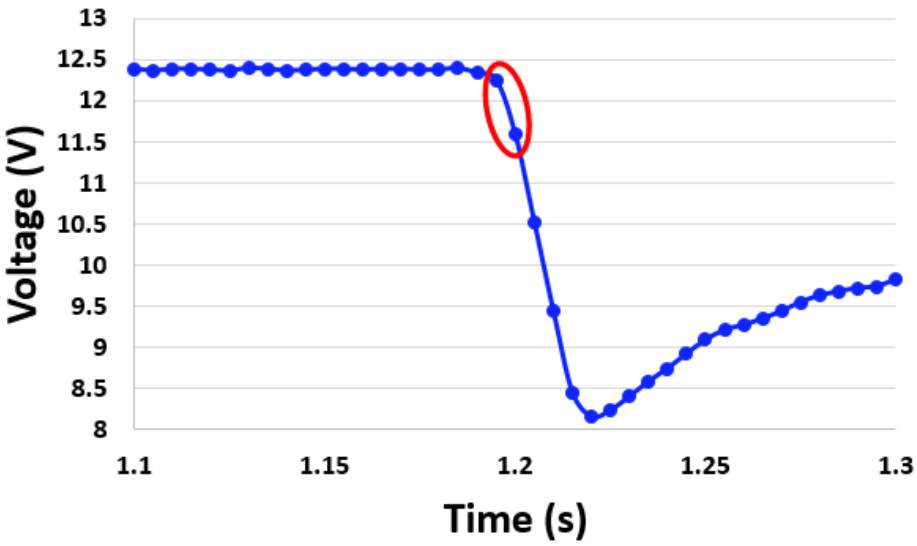

Figure 26: Voltage waveform zoomed from Figure 25 for cranking detection.

Once engine cranking is detected, the MCU processes the average voltage samples to detect the first two valley voltages of a cranking waveform. The algorithm finds a valley voltage with five consecutive average voltage samples (V_1, V_2, V_3, V_4, and V_5) with the following conditions: $V_1 > V_2 \geq V_3 \leq V_4 < V_5$), so V_3 will be the valley voltage. The algorithm finds the first valley voltage followed by the second valley voltage. This valley detection method identified every valley voltages of all battery tests.

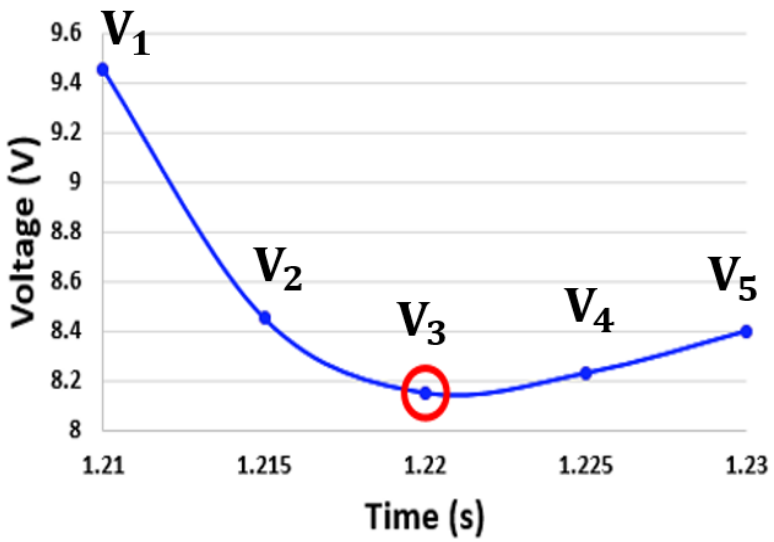

Figure 27: Valley voltage with cranking voltage waveform from Figure 25.

4.3.4 Battery SOH Estimation

When the first two valley voltages are identified, the battery SOH estimation is carried out with OCV, temperature, SOC, first two valley voltages. The sum of the three threshold values, $V_{th} = V_{th1} + V_{th2} + V_{th3}$, is compared with a ΔV_2. With the proposed SOH estimation algorithm, a battery is estimated to be healthy if the SOH metric, $\Delta V_2 - V_{th}$, is positive. It is expected that the SOH metric will decrease over the aging period since the value of V_{th1} increases with the age of a battery.

5 Measurement Results

This chapter shows the measurement results tested with three new and seven refurbished batteries as well as the power dissipation of the stand-alone prototype. Test results with the proposed SOH estimation method compared to other existing methods are also described in this chapter.

5.1 Power Dissipation

Because the proposed SOH estimation system operates in the sleep state most of the time, the stand-alone prototype dissipates approximately 144 mW during an active state and 36 mW during a sleep state as shown in Figure 28. For a fully charged small lead-acid battery, the developed SOH estimation system with the stand-alone prototype lasts more than a year without charging the battery since a standard small car battery has a capacity of 45 Ah [30]. Considering the self-discharge rate of a lead-acid battery, the power dissipation of the prototype is insignificant [2].

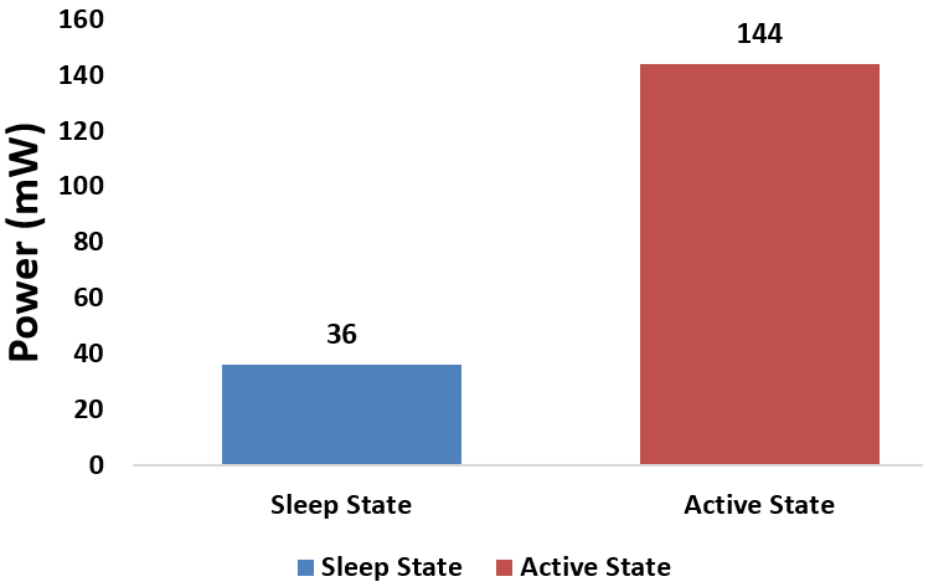

Figure 28: Power dissipation of stand-alone prototype.

5.2 Battery Test Results

Figure 29 shows battery test results of the three new batteries tested with the proposed SOH estimation algorithm. When the SOH metric belongs to the area highlighted in red, below 0 V, it means that the battery is considered unhealthy. As shown in Figure 29, the proposed method predicts the battery failure 1 to 2 weeks before actual battery failure. It should be noted that all the battery test results in this research work are obtained through accelerated battery aging. Without any accelerated battery aging, the algorithm should provide more data points where SOH metrics are negative near the end of battery life. With the proposed algorithm, the prototype gives a low SOH warning if four consecutive SOH metrics are negative. In such a way, any outlier that is not consistent with the general trend of SOH estimation is not included when giving the low SOH warning. SOH metrics of all ten batteries near the end of battery life were negative as shown in Appendix A.

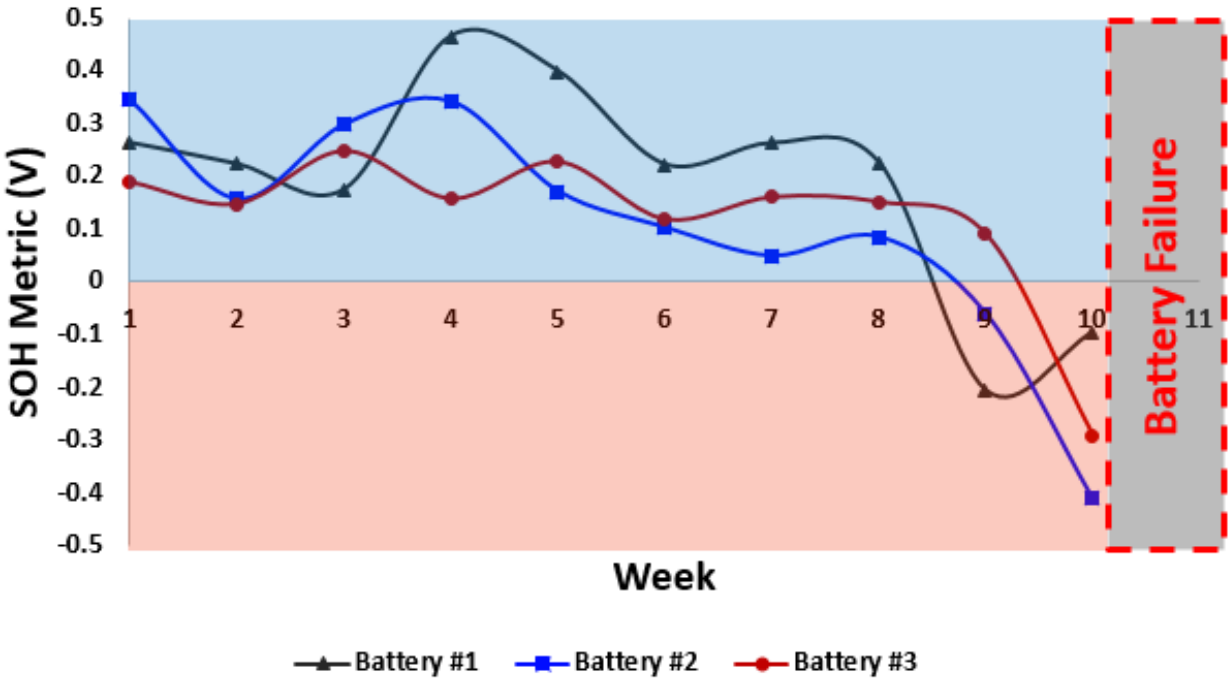

Figure 29: Battery test results of three new batteries with the proposed algorithm.

The batteries were also tested with a commercial battery tester, PBT-300 by Midtronics, to test the condition of the batteries before each engine cranking is performed. The PBT-300 can provide warnings if a battery is healthy (OK), low in battery charge (LOW), or unhealthy (X) as shown in Table 2 below.

Table 2: Battery test results of ten batteries with the PBT-300 by Midtronics.

Period	Battery #1	Battery #2	Battery #3	Battery #4	Battery #5	Battery #6	Battery #7	Battery #8	Battery #9	Battery #10
Week 1	OK	LOW	OK	X	LOW	X	OK	OK	OK	LOW
Week 2	OK	OK	LOW	X	OK	X	OK	LOW	OK	OK
Week 3	OK	LOW	OK	Failed	OK	Failed	OK	LOW	OK	OK
Week 4	LOW	OK	OK		OK		OK	X	OK	LOW
Week 5	LOW	OK	LOW		Failed		Failed	Failed	Failed	LOW
Week 6	OK	OK	OK							OK
Week 7	OK	X	OK							OK
Week 8	OK	X	X							X
Week 9	OK	X	X							X
Week 10	OK	X	X							Failed
Week 11	Failed	Failed	Failed							

Table 3 lists SOH values of three new batteries and seven refurbished batteries, and it compares the proposed method to existing cranking voltage based SOH estimation methods with the measurement data obtained in this work. A cell highlighted in red means that the battery is estimated to be unhealthy with a particular battery SOH estimation method applied to the column. Based on Table 2 and Table 3, it can be observed that the proposed method provides a better failure prediction near the actual time of battery failure than the commercial battery tester and the other two methods except battery #4. The second valley voltage was lower than the first valley voltage for battery #4, and all three methods estimated that this particular battery is unhealthy for the entire periods. The existing cranking voltage methods fail to estimate the battery SOH correctly since they are based on a fully charged battery.

Table 3: SOH values of ten batteries with the measurement data obtained in this work.

	Battery #1 (This work)			Battery #2 (This work)		
Period	ΔV2 (Grube)	SOH Metric (Kerley)	SOH Metric (This work)	ΔV2 (Grube)	SOH Metric (Kerley)	SOH Metric (This work)
Week 1	0.25	-0.03	0.26	0.32	0.03	0.34
Week 2	0.16	-0.11	0.22	0.24	-0.07	0.16
Week 3	0.02	-0.18	0.17	0.10	-0.06	0.30
Week 4	0.14	0.01	0.47	0.27	0.09	0.34
Week 5	0.15	0.00	0.40	0.24	0.09	0.17
Week 6	0.16	0.04	0.22	0.25	0.08	0.10
Week 7	0.16	-0.02	0.26	0.13	-0.08	0.05
Week 8	0.19	-0.02	0.23	0.24	0.06	0.08
Week 9	-0.24	-0.41	-0.21	0.19	-0.08	-0.06
Week 10	0.14	-0.17	-0.10	-0.15	-0.51	-0.41
Week 11	Failed	Failed	Failed	Failed	Failed	Failed
	Battery #3 (This work)			Battery #4 (This work)		
Period	ΔV2 (Grube)	SOH Metric (Kerley)	SOH Metric (This work)	ΔV2 (Grube)	SOH Metric (Kerley)	SOH Metric (This work)
Week 1	0.23	-0.07	0.19	-0.04	-0.35	-0.10
Week 2	0.01	-0.28	0.15	0.00	-0.25	-0.26
Week 3	0.15	-0.07	0.25	Failed	Failed	Failed
Week 4	0.07	-0.10	0.16			
Week 5	0.01	-0.15	0.23			
Week 6	0.16	-0.02	0.12			
Week 7	0.17	0.02	0.16			
Week 8	0.26	0.05	0.15			
Week 9	0.18	-0.04	0.09			
Week 10	0.13	-0.22	-0.29			
Week 11	Failed	Failed	Failed			
	Battery #5 (This work)			Battery #6 (This work)		
Period	ΔV2 (Grube)	SOH Metric (Kerley)	SOH Metric (This work)	ΔV2 (Grube)	SOH Metric (Kerley)	SOH Metric (This work)
Week 1	0.07	-0.21	0.17	0.08	-0.21	0.15
Week 2	0.17	-0.05	0.16	0.11	-0.14	-0.01
Week 3	0.16	-0.02	0.17	Failed	Failed	Failed
Week 4	0.02	-0.21	-0.38			
Week 5	Failed	Failed	Failed			

	Battery #7 (This work)			Battery #8 (This work)		
Period	ΔV2 (Grube)	SOH Metric (Kerley)	SOH Metric (This work)	ΔV2 (Grube)	SOH Metric (Kerley)	SOH Metric (This work)
Week 1	0.30	0.01	0.24	0.10	-0.06	0.23
Week 2	0.08	-0.08	0.13	0.18	0.02	0.37
Week 3	0.10	-0.07	0.19	0.20	0.02	0.30
Week 4	0.08	-0.10	-0.03	-0.04	-0.28	-0.01
Week 5	Failed	Failed	Failed	Failed	Failed	Failed
	Battery #9 (This work)			Battery #10 (This work)		
Period	ΔV2 (Grube)	SOH Metric (Kerley)	SOH Metric (This work)	ΔV2 (Grube)	SOH Metric (Kerley)	SOH Metric (This work)
Week 1	0.34	0.03	0.14	0.24	-0.05	0.24
Week 2	0.12	-0.06	0.06	0.09	-0.11	0.14
Week 3	0.25	0.08	0.32	0.21	0.05	0.28
Week 4	-0.79	-0.96	-1.03	0.21	0.06	0.44
Week 5	Failed	Failed	Failed	0.12	-0.05	0.26
Week 6				0.22	0.02	0.22
Week 7				0.37	0.20	0.24
Week 8				0.15	-0.07	-0.12
Week 9				0.04	-0.29	-0.19
Week 10				Failed	Failed	Failed

Since all the new batteries failed to start a car after 10 weeks of battery aging, each period of battery is equivalent to five to six months of actual battery usage as new automotive lead-acid batteries last four to five years [18].

Table 4 compares SOH values of ten batteries estimated with Kerley's method and estimated with the proposed method based on the measurement data obtained by Kerley [11]. As shown in the table below, the proposed method can provide a better failure prediction for battery #5 and battery #11 than the Grube's method. Similarly, the proposed method provided a better failure prediction for batteries #1, #5, #9, and #11.

Table 4: SOH values of ten batteries with the measurement data from Kerley [11].

	Battery #1 (Kerley)			Battery #4 (Kerley)		
Period	ΔV2 (Grube)	SOH Metric (Kerley)	SOH Metric (This work)	ΔV2 (Grube)	SOH Metric (Kerley)	SOH Metric (This work)
Week 1	0.93	0.55	0.16	0.51	0	-0.37
Week 2	0.98	0.46	0.05	1.19	0.64	0.24
Week 3	0.36	-0.03	-0.40	0.61	0.18	-0.27
Week 4	0.63	0.22	-0.18	0.11	-0.36	-0.88
Week 5	Failed	Failed	Failed	Failed	Failed	Failed
	Battery #5 (Kerley)			Battery #6 (Kerley)		
Period	ΔV2 (Grube)	SOH Metric (Kerley)	SOH Metric (This work)	ΔV2 (Grube)	SOH Metric (Kerley)	SOH Metric (This work)
Week 1	1.03	0.53	0.14	0.92	0.49	0.00
Week 2	0.90	0.22	-0.18	0.58	0.05	-0.42
Week 3	Failed	Failed	Failed	0.65	0.05	-0.50
Week 4				0.56	0.14	-0.43
Week 5				0.44	-0.05	-0.71
Week 6				-0.14	-0.57	-1.23
Week 7				Failed	Failed	Failed
	Battery #7 (Kerley)			Battery #8 (Kerley)		
Period	ΔV2 (Grube)	SOH Metric (Kerley)	SOH Metric (This work)	ΔV2 (Grube)	SOH Metric (Kerley)	SOH Metric (This work)
Week 1	0.91	0.77	0.22	0.99	0.62	0.04
Week 2	0.86	0.39	0.12	0.43	-0.01	-0.69
Week 3	0.09	-0.31	-0.59	Failed	Failed	Failed
Week 4	0.06	-0.28	-0.60			
Week 5	0.20	-0.14	-0.49			
Week 6	Failed	Failed	Failed			
	Battery #9 (Kerley)			Battery #11 (Kerley)		
Period	ΔV2 (Grube)	SOH Metric (Kerley)	SOH Metric (This work)	ΔV2 (Grube)	SOH Metric (Kerley)	SOH Metric (This work)
Week 1	0.44	-0.07	-0.45	0.84	0.28	-0.28
Week 2	0.54	0.16	-0.29	Failed	Failed	Failed
Week 3	0.52	0.10	-0.42			
Week 4	0.08	-0.28	-0.74			
Week 5	Failed	Failed	Failed			
	Battery #12 (Kerley)			Battery #13 (Kerley)		
Period	ΔV2 (Grube)	SOH Metric (Kerley)	SOH Metric (This work)	ΔV2 (Grube)	SOH Metric (Kerley)	SOH Metric (This work)
Week 1	0.37	-0.06	-0.32	0.81	0.33	0.01
Week 2	0.33	-0.16	-0.41	Failed	Failed	Failed
Week 3	0.06	-0.27	-0.58			
Week 4	Failed	Failed	Failed			

6 Conclusion

The proposed SOH estimation method presented in this thesis addresses the shortcomings of existing cranking voltage based SOH estimation methods by considering the SOC of a battery in addition to initial voltage drop, first two valley voltages, and temperature. Because the existing cranking voltage based battery SOH estimation methods are based on a fully charged battery, the estimation methods become unreliable as the battery SOC is low. The proposed algorithm uses three individual threshold voltages from ΔV_1, SOC, and temperature for a reliable SOH estimation. With the proposed SOH estimation method, a battery is considered healthy if ΔV_2 is greater than the sum of the threshold voltages.

The measured data for the SOH estimation were obtained through accelerated battery aging and battery cranking tests with three new batteries and seven refurbished batteries. The development of the three individual threshold voltages based on the collected data is explained in this thesis. For this work, the SOC of a battery is estimated with battery open-circuit voltage and temperature.

To validate and test the proposed battery SOH estimation method, two hardware prototypes implementing the proposed algorithm have been developed. The prototypes are designed to implement the proposed method and algorithm with low power consumption for actual automotive applications without any battery drain concerns. The prototypes can estimate the health of a battery during engine cranking and provide a low SOH warning for an unhealthy battery to prevent a sudden battery failure. A low SOC warning is also provided by the prototypes if the battery SOC is less than 40% so the battery can be charged for a better cranking ability.

A low power ARM Cortex-M4F based MCU included in the prototype implements the proposed SOH algorithm. The power dissipation of the stand-alone prototype is approximately 144 mW during an active state and 36 mW during a sleep state. The MCU is in the sleep state except the time when the MCU enters its active state due to a door activity for the SOH estimation. Any accelerations due to the door activity can be detected by the accelerometer when a user opens or closes the car door, and it will wake up the MCU to enter its active state.

The measurement results show that the proposed SOH estimation method is more effective in estimating the health of a battery and predicting battery failure than existing cranking voltage based SOH estimation methods. It is important to remind that the developed system does not require a costly current sensor for the battery SOH estimation, which makes the system more cost-effective than commercial battery testers. With such low power dissipation and reliable SOH estimation, the proposed SOH estimation system is suitable for an on-board battery monitoring as currently there is no on-board warning that can prevent a sudden battery failure in modern cars. Replacing an unhealthy battery with a low SOH warning on schedule can reduce unnecessary battery maintenance costs.

Future research work to improve the proposed SOH estimation algorithm includes incorporating charging and discharging history as well as the depth of battery discharging to keep track of the battery degradation. The fine-tuning of the threshold voltages with more battery tests should also help develop more reliable and robust SOH estimation algorithm. This SOH estimation method can be also extended for other types of batteries, such as lithium-ion batteries, for electric or hybrid cars.

Bibliography

[1] V. Rich, *The International Lead Trade*. Cambridge, England: Woodhead Publishing, 1994.

[2] T. Reddy, *Linden's Handbook of Batteries*, 4th ed. New York, NY: McGraw-Hill, 2011.

[3] R. Baxter, *Energy Storage: A Nontechnical Guide*. Tulsa, Oklahoma: PennWell Corporation, 2005, pp. 108-110.

[4] S. T. Moeller, *Energy Efficiency: Issues and Trends*. Hauppauge, NY: Nova Science Publishers, INC., 2002.

[5] D. Le and X. Tang, "Lithium-ion Battery State of Health Estimation Using Ah-V Characterization," in *Annual Conference of the Prognostics and Health Management Society*, 2011, pp. 367–73.

[6] S. Bennett, *Heavy Duty Truck Systems*, 5th ed. Clifton Park, NY: Delmar Cengage Learning, 2010.

[7] B. V. Ratnakumar, M. C. Smart and S. Surampudi, "Electrochemical impedance spectroscopy and its applications to lithium ion cells," *The Seventeenth Annual Battery Conference on Applications and Advances*, 2002. Long Beach, CA, 2002, pp. 273-277.

[8] R. Grube, "Automotive Battery State-Of-Health Monitoring Methods," Master of Science in Engineering, Wright State University, 2008.

[9] H. Blanke, O. Bohlen, S. Buller, R. W. De Doncker, B. Fricke, A. Hammouche, D. Linzen, M. Thele, and D. U. Sauer, "Impedance measurements on lead–acid batteries for state-of-charge, state-of-health and cranking capability prognosis in electric and hybrid electric vehicles," *Journal of Power Sources*, vol. 144, no. 2, pp. 418–425, Jun. 2005.

[10] Thanh-Tuan Nguyen, Van-Long Tran and Woojin Choi, "Development of the intelligent charger with battery State-Of-Health estimation using online impedance spectroscopy," *2014 IEEE 23rd International Symposium on Industrial Electronics (ISIE)*, Istanbul, 2014, pp. 454-458.

[11] R. Kerley, "Automotive Lead-Acid Battery State-of-Health Monitoring System," Master of Science in Engineering, Virginia Tech, 2014.

[12] R. Kerley, J. H. Hyun and D. S. Ha, "Automotive lead-acid battery state-of-health monitoring system," *IECON 2015 - 41st Annual Conference of the IEEE Industrial Electronics Society*, Yokohama, 2015, pp. 3934-3938.

[13] D. Xu, X. Huo, X. Bao, C. Yang, H. Chen and B. Cao, "Improved EKF for SOC of the storage battery," *2013 IEEE International Conference on Mechatronics and Automation*, Takamatsu, 2013, pp. 1497-1501.

[14] D. Pavlov, *Lead-Acid Batteries: Science and Technology: A handbook of lead-acid battery technology and its influence on the product*. Amsterdam, Singapore: Elsevier Science Ltd., 2011.

[15] T. L. Churchill, J. S. Edmonds and C. T. Feyk, "Comprehensive noninvasive battery monitoring of lead-acid storage cells in unattended locations," *The 16th International Telecommunications Energy Conference*, Vancouver, BC, 1994, pp. 594-601.

[16] D. Knowles, *TechOne: Basic Automotive Service & Maintenance*. Clifton Park, NY: Delmar Cengage Learning, 2004.

[17] Texas Instruments, "Tiva C Series TM4C123G LaunchPad." [Online]. Available: http://www.ti.com/tool/ek-tm4c123gxl. [Accessed: 30-May-2016].

[18] T. R. Crompton, *Battery Reference Book*, 3rd ed. Woburn, MA: Newnes, 2000.

[19] "SAE J240 Life Test for Automotive Storage Batteries." SAE International, Dec. 2012.

[20] Tempco, "Tempco Over-the-Side Immersion Heaters." [Online]. Available: http://www.tempco.com/Tubular%20Process/Tank%20Heaters/Over%20the%20Side%20Heater.htm. [Accessed: 30-May-2016].

[21] Texas Instruments, "MSP430G2553 Mixed Signal Microcontroller." [Online]. Available: http://www.ti.com/product/MSP430G2553. [Accessed: 30-May-2016].

[22] STMicroelectronics, "VN5E010MH-E Single-channel high-side driver with analog current sense for automotive applications." [Online]. Available: http://www.st.com/web/en/resource/technical/document/datasheet/CD00233832.pdf. [Accessed: 30-May-2016].

[23] Digilent, "Analog Discovery 100MSPS USB Oscilloscope & Logic Analyzer." [Online]. Available: http://store.digilentinc.com/analog-discovery-100msps-usb-oscilloscope-logic-analyzer/. [Accessed: 30-May-2016].

[24] Amprobe, "TMD-56 Multi-logging Digital Thermometer." [Online]. Available: http://www.amprobe.com/amprobe/usen/hvac-tools/thermocouple-thermometers/amp-tmd-56.htm?pid=73414. [Accessed: 30-May-2016].

[25] Midtronics, "Midtronics PBT-300 Professional Battery Tester." [Online]. Available: http://www.midtronics.com/shop/products-1/battery-and-electrical-system-diagnostics/pbt-series-battery-and-electrical-system-testers/midtronics-pbt-300-professional-battery-tester. [Accessed: 30-May-2016].

[26] Linear Technology, “LTC3631 - High Efficiency, High Voltage 100mA Synchronous Step-Down Converter.” [Online]. Available: http://www.linear.com/product/LTC3631. [Accessed: 1-June-2016].

[27] Texas Instruments, “TM4C123GH6PM Tiva C Series TM4C123GH6PM Microcontroller.” [Online]. Available: http://www.ti.com/lit/ds/spms376e/spms376e.pdf. [Accessed: 1-June-2016].

[28] Analog Devices, “ADXL345 - 3-Axis Digital Accelerometer.” [Online]. Available: http://www.analog.com/en/products/mems/mems-accelerometers/adxl345.html#product-overview. [Accessed: 1-June-2016].

[29] Texas Instruments, “LM34 Precision Fahrenheit Temperature Sensors.” [Online]. http://www.ti.com/lit/ds/symlink/lm34.pdf. [Accessed: 1-June-2016].

[30] P. Bures, *America: The Oil Hostage*. College Station, TX: Virtualbookworm.com Publishing, 2006.

Appendix A: Battery Measurements and Test Results

Battery #	Test #	Date (mm/dd/yy)	°C	OCV (V)	SOC (%)	V_1 (V)	V_2 (V)	ΔV_1 (V)	ΔV_2 (V)	V_{th} (V)	SOH Metric (V)
1	1	09/14/14	22.4	12.29	50	10.70	10.95	1.59	0.25	-0.01	0.26
	2	09/27/14	26.8	12.22	40	10.76	10.92	1.46	0.16	-0.06	0.22
	3	10/04/14	13.5	12.28	50	10.90	10.92	1.38	0.02	-0.15	0.17
	4	10/31/14	5.5	12.10	25	10.58	10.72	1.52	0.14	-0.33	0.47
	5	11/12/14	7.4	12.13	30	10.49	10.64	1.64	0.15	-0.25	0.40
	6	11/18/14	4.3	12.46	76	10.85	11.01	1.62	0.16	-0.06	0.22
	7	11/24/14	10.2	12.33	57	10.75	10.91	1.58	0.16	-0.10	0.26
	8	12/01/14	12.0	12.34	58	10.63	10.82	1.71	0.19	-0.04	0.23
	9	12/07/14	7.8	12.37	63	10.57	10.33	1.80	-0.24	-0.03	-0.21
	10	04/04/15	23.5	12.53	83	10.69	10.82	1.84	0.14	0.23	-0.10
	11	04/10/15	17.7	12.25	42						Failed
2	1	09/14/14	22.6	12.20	37	10.43	10.75	1.76	0.32	-0.03	0.34
	2	09/27/14	27.3	12.23	40	10.26	10.50	1.97	0.24	0.08	0.16
	3	10/31/14	5.8	12.13	30	10.26	10.35	1.87	0.10	-0.20	0.30
	4	11/06/14	7.2	12.23	43	10.18	10.45	2.05	0.27	-0.07	0.34
	5	11/12/14	4.5	12.49	80	10.50	10.74	1.99	0.24	0.07	0.17
	6	11/18/14	5.7	12.55	87	10.44	10.69	2.11	0.25	0.15	0.10
	7	11/24/14	9.8	12.35	60	10.17	10.30	2.18	0.13	0.08	0.05
	8	11/30/14	5.4	12.46	76	10.11	10.35	2.34	0.24	0.15	0.08
	9	12/07/14	8.0	12.26	47	9.16	9.35	3.10	0.19	0.25	-0.06
	10	03/28/15	23.4	12.25	44	9.63	9.47	2.65	-0.15	0.42	-0.41
	11	04/04/15	20.6	12.41	65						Failed
3	1	09/14/14	22.2	12.27	47	10.43	10.66	1.84	0.23	0.04	0.19
	2	09/27/14	26.9	12.00	7	10.22	10.23	1.78	0.01	-0.14	0.15
	3	10/04/14	13.3	12.25	45	10.57	10.72	1.68	0.15	-0.10	0.25
	4	10/31/14	7.7	12.29	52	10.48	10.55	1.81	0.07	-0.09	0.16
	5	11/06/14	6.2	12.10	25	10.21	10.22	1.89	0.01	-0.22	0.23
	6	11/12/14	6.7	12.39	65	10.31	10.47	2.08	0.16	0.04	0.12
	7	11/18/14	4.7	12.38	65	10.33	10.50	2.05	0.17	0.01	0.16
	8	11/24/14	9.9	12.39	65	10.20	10.46	2.19	0.26	0.11	0.15
	9	12/07/14	8.3	12.30	53	9.90	10.08	2.40	0.18	0.09	0.09
	10	04/04/15	23.7	12.47	75	9.82	9.95	2.65	0.13	0.42	-0.29
	11	04/10/15	17.5	12.32	52						Failed
4	1	09/27/14	27.1	12.19	35	10.20	10.16	1.99	-0.04	0.06	-0.10

	2	10/04/14	13.5	12.56	87	10.36	10.36	2.20	0.00	0.26	-0.26
	3	10/31/14	6.2	12.66	95						Failed
5	1	09/27/14	27.5	12.12	25	10.54	10.61	1.58	0.07	-0.10	0.17
	2	10/04/14	14.2	12.45	73	10.93	11.10	1.52	0.17	0.01	0.16
	3	11/12/14	7.9	12.34	59	10.38	10.54	1.96	0.16	-0.01	0.17
	4	11/18/14	4.9	12.51	83	9.39	9.41	3.12	0.02	0.40	-0.38
	5	11/24/14	9.6	12.30	48						Failed
6	1	09/27/14	26.3	12.11	24	10.37	10.45	1.74	0.08	-0.07	0.15
	2	10/04/14	16.2	12.5	80	10.79	10.90	1.71	0.11	0.12	-0.01
	3	10/31/14	6.5	10.54	0						Failed
7	1	09/21/14	27.2	12.26	45	10.47	10.77	1.79	0.30	0.06	0.24
	2	11/06/14	7.8	12.41	68	10.74	10.82	1.67	0.08	-0.05	0.13
	3	11/12/14	7.1	12.27	49	10.39	10.49	1.88	0.10	-0.09	0.19
	4	11/18/14	7.7	12.52	83	10.55	10.63	1.97	0.08	0.11	-0.03
	5	11/24/14	9.1	12.27	44						Failed
8	1	10/31/14	7.5	12.26	47	10.49	10.59	1.77	0.10	-0.13	0.23
	2	11/06/14	6.6	12.15	32	10.31	10.49	1.84	0.18	-0.19	0.37
	3	11/12/14	7.1	12.18	37	10.13	10.33	2.05	0.20	-0.10	0.30
	4	11/24/14	11	12.15	32	9.90	9.86	2.25	-0.04	-0.03	-0.01
	5	11/30/14	5.3	6.99	0						Failed
9	1	09/21/14	27.5	12.28	47	10.25	10.59	2.03	0.34	0.14	0.20
	2	10/31/14	8.5	12.48	78	10.64	10.76	1.84	0.12	0.06	0.06
	3	11/06/14	6.9	12.23	43	10.17	10.42	2.06	0.25	-0.07	0.32
	4	11/18/14	4.1	12.72	100	10.46	9.67	2.26	-0.79	0.24	-1.03
	5	11/24/14	9.8	5.28	0						Failed
10	1	09/21/14	27.1	12.20	37	10.46	10.70	1.74	0.24	0.00	0.24
	2	10/04/14	12.4	12.39	65	10.85	10.94	1.54	0.09	-0.05	0.14
	3	10/31/14	8.0	12.37	63	10.72	10.93	1.65	0.21	-0.07	0.28
	4	11/06/14	6.3	12.14	31	10.42	10.63	1.72	0.21	-0.23	0.44
	5	11/12/14	7.6	12.20	39	10.34	10.46	1.86	0.12	-0.14	0.26
	6	11/24/14	9.1	12.32	56	10.33	10.55	1.99	0.22	0.00	0.22
	7	11/30/14	5.3	12.52	83	10.39	10.76	2.13	0.37	0.13	0.24
	8	12/07/14	7.9	12.51	82	9.96	10.11	2.55	0.15	0.27	-0.12
	9	03/28/15	20.8	12.39	63	10.13	10.17	2.26	0.04	0.23	-0.19
	10	04/04/15	21.4	10.39	0						Failed

Appendix B: List of Batteries

Battery #	Battery Manufacturer	Battery Description	Note
1	AutoCraft Batteries	AutoCraft Gold Battery, Group Size 86, 640 CCA	This battery was purchased as new, and it failed after 10 successful cranks.
2	AutoCraft Batteries	AutoCraft Silver Battery, Group Size 86, 525 CCA	This battery was purchased as new, and it failed after 10 successful cranks.
3	Duralast Batteries	Duralast Battery, Group Size 86, 525 CCA	This battery was purchased as new, and it failed after 10 successful cranks.
4	Interstate Batteries	Econo Power, Group Size 86, 525 CCA	This battery was purchased as refurbished, and it failed after 2 successful cranks.
5	Interstate Batteries	Econo Power, Group Size 86, 525 CCA	The battery was purchased as refurbished, and it failed after 4 successful cranks.
6	Interstate Batteries	Econo Power, Group Size 86, 525 CCA	The battery was purchased as refurbished, and it failed after 2 successful cranks.
7	Interstate Batteries	Econo Power, Group Size 86, 525 CCA	The battery was purchased as refurbished, and it failed after 4 successful cranks.
8	Interstate Batteries	Econo Power, Group Size 86, 525 CCA	The battery was purchased as refurbished, and it failed after 4 successful cranks.
9	Interstate Batteries	Econo Power, Group Size 86, 525 CCA	The battery was purchased as refurbished, and it failed after 4 successful cranks.
10	Interstate Batteries	Econo Power, Group Size 86, 525 CCA	The battery was purchased as refurbished, and it failed after 9 successful cranks.